

Elsevier Editorial System(tm) for Antiviral Research
Manuscript Draft

Manuscript Number:

Title: Nasal chitosan microparticles to target zidovudine prodrug to brain HIV sanctuaries

Article Type: Research Paper

Section/Category: HIV and other retroviruses

Keywords: Zidovudine prodrug; HIV treatment; macrophages; brain targeting; nasal formulation; chitosan microparticles

Corresponding Author: Dr. Giovanna Rassu, PhD

Corresponding Author's Institution: University of Sassari

First Author: Alessandro Dalpiaz

Order of Authors: Alessandro Dalpiaz ; Marco Fogagnolo ; Luca Ferraro ; Antonio Capuzzo ; Barbara Pavan ; Giovanna Rassu, PhD; Andrea Salis; Paolo Giunchedi; Elisabetta Gavini

Manuscript Region of Origin: ITALY

Abstract: Zidovudine (AZT) is an antiretroviral drug substrate of active efflux transporters (AET) that extrude it from the central nervous system (CNS) and macrophages, considered sanctuaries of HIV. The conjugation of AZT with ursodeoxycholic acid is known to produce a prodrug (UDCA-AZT) able to elude the AET systems, evidencing the potential ability of this prodrug to act as a carrier of AZT in the CNS and macrophages. Here, we demonstrate that UDCA-AZT is able to permeate and remain in murine macrophages with an efficiency twenty times higher than AZT. Moreover, we propose the nasal administration of this prodrug in order to induce its CNS uptake. Chitosan chloride based microparticles (CP) were prepared by spray-drying and characterized for size, morphology, density, water uptake and dissolution profile of UDCA-AZT. The CP sample was then nasally administered to rats. All in-vitro and in-vivo measurements were achieved also for a CP parent physical mixture. The CP sample was able to increase the dissolution rate of UDCA-AZT and to reduce water uptake with respect to its parent physical mixture, inducing a better uptake of UDCA-AZT in the cerebrospinal fluid of rats, where the prodrug can act as an AZT carrier in the macrophages.

Suggested Reviewers: Jared Fine

Center for Memory and Aging, Health Partners Institute for Education and Research, Saint Paul
jared.m.fine@healthpartners.com
expert in nose to brain delivery of drug

Marta Roldo

School of Pharmacy and BMS, Portsmouth
marta.roldo@port.ac.uk
expert in drug delivery

Alessio Cardinale
1IRCCS San Raffaele Pisana, Rome, Italy
alessio.cardinale@sanraffaele.it
Expert in biological aspects of brain diseases

Sassari, July 7, 2015

Dear Editor,

please find as attached file the original manuscript entitled “Influence of chitosan chloride microparticles on the *in vivo* intranasal uptake of a zidovudine prodrug for brain targeting” by A. Dalpiaz, M. Fogagnolo, L. Ferraro, A. Capuzzo, B. Pavan, G. Rassu, A. Salis, P. Giunchedi, E. Gavini.

In order to study new strategies potentially able to enhance the brain targeting of zidovudine (AZT), this manuscript describes the design and formulation of chitosan based microparticles (CP) as a carrier system for the nasal administration of a prodrug obtained by conjugation with ursodeoxycholic acid. We characterize *in vitro* the CP sample and its parent physical mixture and we demonstrate that their nasal administration to rats allows to obtain the prodrug uptake in their cerebrospinal fluid. We also evidence for the first time that the uptake of UDCA-AZT in murine macrophages is definitely higher than that of AZT. We conclude that CP sample appears as an efficacious nasal formulation for the selective uptake in the central nervous system of zidovudine.

We would be grateful if this manuscript could be considered for the publication in *Antiviral Research*. The submission file has been done according to “Author Information Pack”. Nevertheless, as we did a lot of experimental work, and despite we tried to shorten, the length of the manuscript is 5921 words, excluded the references. We would you like to know if the manuscript is nonetheless worthy to be considered for the submission.

Finally, I confirm that all authors have read and approved this version of the article, and no part of this paper has been published nor is it submitted for publication elsewhere and will not be submitted elsewhere.

With best regards,

Giovanna Rassu, Ph.D.

Highlights

1
2
3
4
5
6
7
8
9
10
11
12
13
14
15
16
17
18
19
20
21
22
23
24
25
26
27
28
29
30
31
32
33
34
35
36
37
38
39
40
41
42
43
44
45
46
47
48
49
50
51
52
53
54
55
56
57
58
59
60
61
62
63
64
65

- We evidence for the first time that the uptake of prodrug UDCA-AZT in murine macrophages is higher than that of zidovudine.
- Intravenous administration of zidovudine (AZT) and UDCA-AZT is not efficient in brain targeting.
- Nasal administration of physical mixture/microparticles produces detectable amounts of UDCA–AZT in the cerebrospinal fluid.
- Chitosan nasal microspheres show the best performance in UDCA-AZT uptake in cerebrospinal fluid.
- This formulation can induce the AZT transport in macrophages located in the subarachnoid spaces of cerebrospinal fluid.

Nasal chitosan microparticles to target zidovudine prodrug to brain HIV sanctuaries

Alessandro Dalpiaz ^a, Marco Fogagnolo ^a, Luca Ferraro ^b, Antonio Capuzzo ^b, Barbara Pavan ^b,
Giovanna Rassu ^{c,*}, Andrea Salis ^c, Paolo Giunchedi ^c, Elisabetta Gavini ^c

^a*Department of Chemical and Pharmaceutical Sciences, University of Ferrara, via Fossato di
Mortara 19, 44121 Ferrara, Italy*

^b*Department of Life Sciences and Biotechnology, University of Ferrara, via Borsari 46, 44121
Ferrara, Italy*

^c*Department of Chemistry and Pharmacy, University of Sassari, via Muroni 23/a, 07100 Sassari,
Italy*

E-mail addresses: dla@unife.it (A. Dalpiaz), marco.fogagnolo@unife.it (M. Fogagnolo),
fri@unife.it (L. Ferraro), antonio.capuzzo@unife.it (A. Capuzzo), pvnbb@unife.it (B. Pavan),
grassu@uniss.it (G. Rassu), asalis@uniss.it (A. Salis), pgiunc@uniss.it (P. Giunchedi),
eligav@uniss.it (E. Gavini).

* Corresponding author: Giovanna Rassu, Department of Chemistry and Pharmacy, University of
Sassari, via Muroni 23/a, 07100 Sassari, Italy. Tel: +39 079228735; Fax: +39 079228733; E-mail
address: grassu@uniss.it

ABSTRACT

Zidovudine (AZT) is an antiretroviral drug substrate of active efflux transporters (AET) that extrude it from the central nervous system (CNS) and macrophages, considered sanctuaries of HIV. The conjugation of AZT with ursodeoxycholic acid is known to produce a prodrug (UDCA-AZT) able to elude the AET systems, evidencing the potential ability of this prodrug to act as a carrier of AZT in the CNS and macrophages. Here, we demonstrate that UDCA-AZT is able to permeate and remain in murine macrophages with an efficiency twenty times higher than AZT. Moreover, we propose the nasal administration of this prodrug in order to induce its CNS uptake. Chitosan chloride based microparticles (CP) were prepared by spray-drying and characterized for size, morphology, density, water uptake and dissolution profile of UDCA-AZT. The CP sample was then nasally administered to rats. All *in-vitro* and *in-vivo* measurements were achieved also for a CP parent physical mixture. The CP sample was able to increase the dissolution rate of UDCA-AZT and to reduce water uptake with respect to its parent physical mixture, inducing a better uptake of UDCA-AZT in the cerebrospinal fluid of rats, where the prodrug can act as an AZT carrier in the macrophages.

Keywords: Zidovudine prodrug, HIV treatment, macrophages, brain targeting, nasal formulation, chitosan microparticles

Chemical compounds studied in this article:

Zidovudine (PubChem CID: 35370)

1. Introduction

The combination antiretroviral therapy (cART) has hugely impacted the management of AIDS, but its efficacy is limited by the poor bioavailability of anti-HIV drugs at viral reservoir sites, such as the central nervous system (CNS) (Cunningham et al., 2000; Kolson and Gonzalez-Scarano, 2000), in particular subarachnoid spaces of cerebrospinal fluid (CSF) containing macrophages, that constitute the only site of HIV replication in the brain (Gherssi-Egea et al., 1996; Cunningham et al., 1997). The lack of drug penetration in these “HIV sanctuaries” is mainly due to the expression on the blood–brain (BBB) and blood–cerebrospinal fluid (BCSFB) barriers of active efflux transporter (AET) (Namanja et al., 2012; Pavan and Dalpiaz, 2011) that induce, *in-vivo*, an asymmetric transport of anti-HIV drugs across these barriers, where the rate of drug efflux from CNS to blood is greater than its influx rate (Wang and Sawchuk, 1995).

We recently proved that the conjugation of zidovudine (AZT, an antiretroviral drug used in cART protocols - De Clercq, 2009) with the bile acid ursodeoxycholic acid (UDCA) allows to obtain a prodrug (UDCA–AZT) able to elude the AET systems (Dalpiaz et al., 2012). We have therefore proposed that this prodrug, when taken up in the CNS, should not be extruded in the bloodstream, being able to elude the AET systems. Accordingly, we have demonstrated that the nasal administration of solid lipid microparticles loaded with the UDCA-AZT prodrug allows to obtain its uptake in the cerebrospinal fluid (CSF) of rats (Dalpiaz et al., 2014). It is currently known that nasal administration constitutes a potentially efficacious way in order to obtain the brain uptake of neuroactive agents (Illum, 2000; Vyas et al., 2005; Fine et al, 2014, 2015). Indeed, the drugs deposited on the olfactory epithelium of the nose can have a direct access to the CNS, in particular the CSF via a transcellular transport through olfactory epithelia cells. The drugs absorbed in the CSF can then diffuse into the interstitial fluid (ISF), from where they can penetrate the brain parenchyma (Illum, 2000, 2004; Thorne and Frey, 2001). Moreover, the drugs deposited on the olfactory epithelium can be transported into the brain parenchyma by olfactory neurons or

1 trigeminal nerves that reach the nasal cavity (Finger et al., 1990; Illum, 2000; Johnson et al., 2010).
2 Finally, the nasally administered drugs can be absorbed in the systemic circulation from the
3 respiratory epithelium (Cho et al, 2014), then they can reach the CNS if they are able to cross the
4
5 BBB (Illum, 2000).
6
7

8
9 In general, appropriate strategies are required in order to improve the brain delivery of drugs,
10 such as the addition of penetration enhancers and mucoadhesive materials to formulations, or the
11 preparation of micro and nanoparticulate delivery systems (Casettari and Illum, 2014; Dalpiaz et al.,
12 2008; Horvát et al., 2009; Mistry et al., 2009; Rassu et al., 2015a). In this regards, chitosan is a
13 polysaccharide derived from alkaline deacetylation of chitin, used in different formulations for nose
14 to brain delivery of drugs (Casettari and Illum, 2014) due to its biocompatibility, nontoxicity and
15 high charge density conferring it mucoadhesive properties (Bernkop-Schnürch and Dünnhaupt,
16 2012; Sinha et al, 2004). Chitosan is poorly soluble in water at physiologic pH values, but it forms
17 salts with inorganic or organic acids, such as hydrochloride and glutamic acid, that are soluble in
18 water and can have better characteristics than chitosan itself, such as mucoadhesiveness and
19 penetration enhancement ability of neuroactive agents in the CNS (Dalpiaz et al., 2008; Gavini et
20 al., 2011; Maestrelli et al., 2004). Chitosan is also characterized by the ability of reversibly open
21 tight junctions, with potential increase of transcellular transport of drugs across the olfactory
22 mucosa (Durhia et al, 2010). Nasal formulation obtained in the presence of water show drawbacks,
23 such as risk of chemical and physical instability and microbiological growth. Also, the residence
24 time of the liquid formulation in the nasal cavity is short as the liquid is often rinsed into the
25 gastrointestinal tract (GIT) or out (Kublik and Vidgren, 1998). These disadvantages can be
26 overcome by using powder-based formulations (Marttin et al., 1997; Rassu et al., 2015b).
27
28
29
30
31
32
33
34
35
36
37
38
39
40
41
42
43
44
45
46
47
48
49
50
51
52

53 The purpose of the present work was firstly to demonstrate that UDCA-AZT can permeate
54 and remain in macrophages more efficiently than its parent drug AZT, then the preparation of
55 microspheres based on chitosan chloride in order to increase the nose-to-brain delivery of UDCA-
56 AZT by using a particulate formulation suitable for nasal administration. Characterization of
57
58
59
60
61
62
63
64
65

1 microparticles was performed *in-vitro* and *in-vivo*. All *in-vitro* and *in-vivo* measurements performed
2 for the loaded microparticles were achieved also for a parent physical mixture of chitosan chloride
3 and UDCA-AZT, in order to verify the efficacy of the microparticulate system on the brain delivery
4 of the prodrug.
5
6
7
8
9

10 **2. Materials and methods**

11 *2.1. Materials*

12
13
14
15
16
17
18
19
20
21
22
23
24 The prodrug UDCA–AZT was synthesized as previously described (Dalpiaz et al., 2012).
25 Chitosan chloride (Protasan UP CL 113, molecular weight and degree of deacetylation of 160000
26 g/mol and 83%, respectively) was purchased from FMC BioPolymer AS (Drammen, Norway).
27
28
29
30
31
32
33
34
35
36
37
38
39
40
41
42
43
44
45
46
47
48
49
50
51
52
53
54
55
56
57
58
59
60
61
62
63
64
65
66
67
68
69
70
71
72
73
74
75
76
77
78
79
80
81
82
83
84
85
86
87
88
89
90
91
92
93
94
95
96
97
98
99
100
101
102
103
104
105
106
107
108
109
110
111
112
113
114
115
116
117
118
119
120
121
122
123
124
125
126
127
128
129
130
131
132
133
134
135
136
137
138
139
140
141
142
143
144
145
146
147
148
149
150
151
152
153
154
155
156
157
158
159
160
161
162
163
164
165
166
167
168
169
170
171
172
173
174
175
176
177
178
179
180
181
182
183
184
185
186
187
188
189
190
191
192
193
194
195
196
197
198
199
200
201
202
203
204
205
206
207
208
209
210
211
212
213
214
215
216
217
218
219
220
221
222
223
224
225
226
227
228
229
230
231
232
233
234
235
236
237
238
239
240
241
242
243
244
245
246
247
248
249
250
251
252
253
254
255
256
257
258
259
260
261
262
263
264
265
266
267
268
269
270
271
272
273
274
275
276
277
278
279
280
281
282
283
284
285
286
287
288
289
290
291
292
293
294
295
296
297
298
299
300
301
302
303
304
305
306
307
308
309
310
311
312
313
314
315
316
317
318
319
320
321
322
323
324
325
326
327
328
329
330
331
332
333
334
335
336
337
338
339
340
341
342
343
344
345
346
347
348
349
350
351
352
353
354
355
356
357
358
359
360
361
362
363
364
365
366
367
368
369
370
371
372
373
374
375
376
377
378
379
380
381
382
383
384
385
386
387
388
389
390
391
392
393
394
395
396
397
398
399
400
401
402
403
404
405
406
407
408
409
410
411
412
413
414
415
416
417
418
419
420
421
422
423
424
425
426
427
428
429
430
431
432
433
434
435
436
437
438
439
440
441
442
443
444
445
446
447
448
449
450
451
452
453
454
455
456
457
458
459
460
461
462
463
464
465
466
467
468
469
470
471
472
473
474
475
476
477
478
479
480
481
482
483
484
485
486
487
488
489
490
491
492
493
494
495
496
497
498
499
500
501
502
503
504
505
506
507
508
509
510
511
512
513
514
515
516
517
518
519
520
521
522
523
524
525
526
527
528
529
530
531
532
533
534
535
536
537
538
539
540
541
542
543
544
545
546
547
548
549
550
551
552
553
554
555
556
557
558
559
560
561
562
563
564
565
566
567
568
569
570
571
572
573
574
575
576
577
578
579
580
581
582
583
584
585
586
587
588
589
590
591
592
593
594
595
596
597
598
599
600
601
602
603
604
605
606
607
608
609
610
611
612
613
614
615
616
617
618
619
620
621
622
623
624
625
626
627
628
629
630
631
632
633
634
635
636
637
638
639
640
641
642
643
644
645
646
647
648
649
650
651
652
653
654
655
656
657
658
659
660
661
662
663
664
665
666
667
668
669
670
671
672
673
674
675
676
677
678
679
680
681
682
683
684
685
686
687
688
689
690
691
692
693
694
695
696
697
698
699
700
701
702
703
704
705
706
707
708
709
710
711
712
713
714
715
716
717
718
719
720
721
722
723
724
725
726
727
728
729
730
731
732
733
734
735
736
737
738
739
740
741
742
743
744
745
746
747
748
749
750
751
752
753
754
755
756
757
758
759
760
761
762
763
764
765
766
767
768
769
770
771
772
773
774
775
776
777
778
779
780
781
782
783
784
785
786
787
788
789
790
791
792
793
794
795
796
797
798
799
800
801
802
803
804
805
806
807
808
809
810
811
812
813
814
815
816
817
818
819
820
821
822
823
824
825
826
827
828
829
830
831
832
833
834
835
836
837
838
839
840
841
842
843
844
845
846
847
848
849
850
851
852
853
854
855
856
857
858
859
860
861
862
863
864
865
866
867
868
869
870
871
872
873
874
875
876
877
878
879
880
881
882
883
884
885
886
887
888
889
890
891
892
893
894
895
896
897
898
899
900
901
902
903
904
905
906
907
908
909
910
911
912
913
914
915
916
917
918
919
920
921
922
923
924
925
926
927
928
929
930
931
932
933
934
935
936
937
938
939
940
941
942
943
944
945
946
947
948
949
950
951
952
953
954
955
956
957
958
959
960
961
962
963
964
965
966
967
968
969
970
971
972
973
974
975
976
977
978
979
980
981
982
983
984
985
986
987
988
989
990
991
992
993
994
995
996
997
998
999
1000

2.2. *Uptake of AZT and UDCA-AZT in macrophages*

The murine macrophage cell line J774A.1 was obtained from the American tissue Type Culture Collection (LGC Standards, Milan, Italy). J774A.1 macrophages were grown as adherently cultured cells in Dulbecco's modified Eagle's medium + Glutamax supplemented with 10% fetal bovine

1 serum (FBS), 100 U/mL penicillin, and 100 µg/mL streptomycin at 37 °C. All cell culture reagents
2 were provided by Invitrogen (Life Technologies, Milan, Italy). Method is reported in detail in
3
4 Supplementary material. Briefly, J774A.1 cells were seeded in 12-well culture plates in a total of
5
6 5×10^5 cells and, when semi-confluent, exposed to the solutions of 100 µM AZT and 100 µM
7
8 UDCA-AZT in growth medium for 30 min. At the end of the treatment, cells were washed and
9
10 lysed. Cell lysates were dried under nitrogen stream, resuspended in methanol and centrifuged to
11
12 remove cell debris. The supernatant (10 µl) was used to measure the levels of the test substrates by
13
14 HPLC analysis. All the values obtained by experiments with J774A.1 cells are the mean of three
15
16 independent experiments.
17
18
19
20
21
22
23

24 2.3. *Preparation of loaded and unloaded chitosan microspheres*

25
26
27
28

29 Chitosan microspheres containing UDCA–AZT (named CP) were prepared by spray-drying
30 method. Chitosan chloride (400 mg) was dissolved in water (15 mL), whereas UDCA–AZT (100
31
32 mg) was dissolved in methanol (35 ml). Drug solution was dispersed into chitosan one (solid
33
34 concentration: 1% w/v of UDCA–AZT and chitosan). Due to the very low solubility of drug, a fine
35
36 suspension was obtained and spray-dried using a mini spray-dryer equipped with a high
37
38 performance cyclone (Büchi B-191, Büchi Labortechnik AG, Switzerland) and with a 0.7 mm two-
39
40 fluid nozzle. The following standard operating conditions were utilized: inlet and outlet
41
42 temperature, 100 °C and 73 °C; spray flow rate, 500 L/h; pump setting, 8% (2.00 mL/min);
43
44 aspirator setting, 90%. Aqueous solutions of chitosan chloride (0.8 % w/v) were sprayed in the
45
46 same conditions to obtain drug empty microspheres (CH). Microparticles were stored in a
47
48 desiccator at room temperature.
49
50
51
52
53
54
55
56
57

58 2.4. *HPLC analysis*

59
60
61
62
63
64
65

1 The quantification of the prodrug UDCA–AZT and its hydrolysis product, AZT was
2 performed by HPLC. The chromatographic apparatus consisted of a modular system (model LC-10
3
4 AD VD pump and model SPD-10A VP variable wavelength UV–vis detector; Shimadzu, Kyoto,
5
6 Japan) and an injection valve with 20 μ L sample loop (model 7725; Rheodyne, IDEX, Torrance,
7
8 CA, USA). Separations were performed at room temperature on a 5 μ m Hypersil BDS C-18 column
9
10 (150 mm \times 4.6 mm i.d; Alltech Italia Srl, Milan, Italy), equipped with a guard column. Data
11
12 acquisition and processing were accomplished with a personal computer using CLASS-VP
13
14 Software, version 7.2.1 (Shimadzu Italia, Milan, Italy). The detector was set at 260 nm. The mobile
15
16 phase consisted of a mixture of water and methanol regulated by a gradient profile programmed as
17
18 follows: isocratic elution with 20% (v/v) MeOH in H₂O for 10 min; then a 1-min linear gradient to
19
20 75% (v/v) MeOH in H₂O; the mobile phase composition was finally maintained at 75% MeOH for
21
22 10 min. After each cycle the column was conditioned with 20% (v/v) MeOH in H₂O for 10 min.
23
24 The flow rate was 1 mL/min. The xanthine derivative 7n-PX was employed as internal standard for
25
26 the analysis of rat blood (see below). The retention times for 7n-PX, AZT and the prodrug
27
28 UDCA–AZT were 6.5, 8.4, and 19.6 min, respectively. The HPLC assay of UDCA-AZT alone was
29
30 performed isocratically with 80% (v/v) MeOH in H₂O. In this case the retention time of UDCA-
31
32 AZT was 4.8 min. The chromatographic precision was evaluated (see Supplementary material).
33
34
35
36
37
38
39
40
41
42
43

44 2.5. *Characterization of microspheres*

45
46
47
48
49 Microspheres prepared were characterized in terms of yield of production, drug content and
50
51 encapsulation efficiency, particle size and particle size distribution, particle morphology, true
52
53 density and water uptake capacity.
54
55
56
57

58 2.5.1. *The yields of production*

59
60
61 The yields of production (YP) were calculated as a percent weight of microspheres obtained
62
63
64
65

1
2
3
4
5
6
7
8
9
10
11
12
13
14
15
16
17
18
19
20
21
22
23
24
25
26
27
28
29
30
31
32
33
34
35
36
37
38
39
40
41
42
43
44
45
46
47
48
49
50
51
52
53
54
55
56
57
58
59
60
61
62
63
64
65

with respect to the initial amounts of UDCA–AZT and chitosan employed for preparation of feed suspension.

2.5.2. UDCA–AZT content in CP

The UDCA-AZT content in the microparticulate powders was determined. The microparticles (about 0.95 mg) were accurately weighed and dissolved in 3 ml of water to whom 300 µl of 0.2% H₃PO₄ was added; the final volume of the solution was adjusted to 10 mL with methanol. Then, 10 µL of filtered solutions (0.45 µm) were injected into the HPLC system for UDCA-AZT assay. The drug loading and entrapment efficiency were calculated according to equations 1 and 2 (Rassu et al., 2014; see Supplementary material).

All the values obtained are the mean of four independent experiments.

2.5.3. Particle size measurement

Size and size distribution of microspheres were analyzed by the light diffraction method using a Coulter LS 100Q (Beckman Coulter Particle Characterization, Miami, FL). A sample (2 mg) of unloaded and drug-loaded microspheres was suspended in silicon oil, sonicated for about 3 s and analyzed. The results reported are the averages of the triplicate averages. As comparison, test was also performed on the physical mixture containing UDCA–AZT and chitosan chloride (87:13 w/w) (MIX) prepared by geometrical dilution with the use of agate and mortar pestle, as well as on chitosan chloride and UDCA-AZT alone, before and after grinding.

2.5.4. Particle morphology

Shape and surface characteristics of powders were studied by scanning electron microscopy (VP-SEM; Zeiss EVO40XVP, Arese, Milan, Italy). The samples were placed on double-sided tape that had previously been secured on aluminum stubs and then analyzed at 18 kV acceleration voltage after gold sputtering, under argon atmosphere.

2.5.5. True Density

True density of microspheres was measured by helium pycnometry (Micromeritics Accupyc II 1340 Analysis system, Peschiera Borromeo, Italy) at 21 °C (Gavini et al., 2012). The density (ρ) of the powder was determined in triplicate for each batch.

2.5.6. Determination of water uptake capacity

The investigation of water uptake capability of CP and CH was carried out with a modified Enslin apparatus as already described by Rassa et al., 2009. Briefly, the dried microspheres were spread uniformly on the paper filter, previously soaked with phosphate buffer pH 6.5. Volume of fluid absorbed from microspheres during the time (0 to 60 min) was recorded. The values (mean of at least 3 experiments) were expressed as μL of fluid absorbed per gram of microspheres during the time. As comparison, the test was also performed using MIX.

2.6. In-vitro release and dissolution studies

The release tests were performed by using the flow-through dissolution method (European Pharmacopoeia, Apparatus 4), using a modified glass cell useful for organic solvent (described in Supplementary material). CP formulation (20 mg) was placed into the glass cell. The dissolution medium, thermostated at 37 ± 0.1 °C was introduced through the bottom of the cell to obtain a suitable continuous flow. Methanol-water blend (70-30 v/v) was used as dissolution medium. The test solution (10 μL) was analyzed by HPLC and the amount of UDCA-AZT released from the microspheres was calculated as a percentage of the initial amount of UDCA-AZT incorporated in the microspheres prior to the dissolution test. As comparison, the test was also performed using MIX. All experiments were performed in at least three replicates.

2.7. *In-vivo* UDCA-AZT administration and quantification

1
2
3
4
5 Male Wistar rats (200–250 g) anaesthetized during the experimental period, received a
6
7 femoral intravenous infusion of 0.1 mg/mL UDCA-AZT dissolved in a medium constituted by 20%
8
9 (v/v) DMSO and 80% (v/v) physiologic solution, with a rate of 0.2 mL/min for 10 min. At the end
10
11 of infusion and at fixed time points, blood samples (100 μ L) were collected and CSF samples (50
12
13 μ L) were withdrawn by cisternal puncture method described by van den Berg et al. (2002)
14
15 requiring a single needle stick and allows the collection of serial (40–50 μ L) CSF samples which
16
17 are virtually blood-free (Dalpiaz et al., 2014). A total volume of about 150 μ L CSF was collected
18
19 during the experimental session. Four rats were employed for femoral intravenous infusions. CSF
20
21 samples (10 μ L) were immediately injected into HPLC system for UDCA-AZT detection. The
22
23 blood samples were hemolysed immediately after their collection with 500 μ L of ice cold water,
24
25 then 50 μ L of 10% sulfosalicylic acid and 100 μ L of internal standard (30 μ M 7n-PX) were added.
26
27 The samples were extracted twice with 1 mL of water saturated ethyl acetate, and, after
28
29 centrifugation, the organic layer was reduced to dryness under a nitrogen stream. Two hundred
30
31 microliters of a water-methanol mixture (70:30 v/v) were added, and, after centrifugation, 10 μ L
32
33 was injected into the HPLC system.
34
35
36
37
38
39
40
41

42 The precision of the analytical method was determined (see Supplementary material). The *in-*
43
44 *vivo* half-life of AZT in the blood was calculated by nonlinear regression (exponential decay) of
45
46 concentration values in the time range within 3 hours after infusion and confirmed by linear
47
48 regression of the log concentration values *versus* time.
49
50
51

52 Nasal administration of UDCA-AZT was performed on anaesthetized rats laid on their backs,
53
54 following two main procedures. The first one consisted of the introduction of 50 μ L of an aqueous
55
56 suspension of UDCA-AZT (2 mg/mL) in each nostril of rats as previously described (Dalpiaz et al.,
57
58 2014). After the administration, blood (100 μ L) and CSF samples (50 μ L) were collected at fixed
59
60
61
62
63
64
65

1
2
3
4
5
6
7
8
9
10
11
12
13
14
15
16
17
18
19
20
21
22
23
24
25
26
27
28
29
30
31
32
33
34
35
36
37
38
39
40
41
42
43
44
45
46
47
48
49
50
51
52
53
54
55
56
57
58
59
60
61
62
63
64
65

time points, and they were analyzed with the same procedures described above. Four rats were employed for nasal administration of UDCA-AZT suspension.

The second procedure was based on the insufflations of CP microparticles to each nostril of anaesthetized rats by single dose Monopowder P[®] insufflators (Valois Dispray SA, Mezzovico, Switzerland). These devices were constituted by a pump, a nasal adapter and a solid formulation reservoir (Sacchetti et al., 2002). The insufflators were loaded with about 0.8 mg UDCA-AZT-loaded microparticles (corresponding to about 100 µg of UDCA-AZT), or with about 0.8 mg the corresponding physical mixture (MIX), and the rats received this amount to each nostril. The amount of powder emitted during administration was obtained by the difference in the insufflator weight before and after each insufflation. After the administration, blood (100 µL) and CSF samples (50 µL) were collected at fixed time points, and they were analyzed with the same procedures described above. Four rats were employed for nasal administration of the microparticulate powder.

All *in-vivo* experiments were performed in accordance with the guidelines issued by the Italian Ministry of Health (D.L. 116/92 and D.L. 111/94-B), the Declaration of Helsinki, and the Guide for the Care and Use of Laboratory Animals as adopted and promulgated by the National Institute of Health (Bethesda, Maryland). The protocol of all the *in-vivo* experiments has been approved by Local Ethics Committee (University of Ferrara, Ferrara, Italy). Any effort has been done to reduce the number of the animals and their suffering.

The area under concentration curves of UDCA-AZT in the CSF (AUC, µg mL⁻¹ min) were calculated by the trapezoidal method. All the calculations were performed by using the computer program Graph Pad Prism (GraphPad Software Incorporated, La Jolla, CA, USA).

2.8. Statistical analysis

Statistical comparisons of the amounts of water uptake of the powder samples or the UDCA-

1 AZT AUC values obtained in the CSF of rats were made by Student's t test or one way ANOVA
2 (GraphPad Prism). $P < 0.05$ was considered statistically significant.
3
4
5
6
7
8

9 **3. Results**

10 *3.1. Uptake of AZT and UDCA-AZT in macrophages*

11
12
13
14
15
16
17
18
19 The incubation of 100 μM zidovudine or its prodrug with the macrophages for 30 min
20 allowed to detect, in 10^6 cells, 0.054 ± 0.007 moles of AZT and 1.12 ± 0.16 moles of UDCA-AZT, as
21 reported in Fig. 1. These data evidence the ability the prodrug to permeate and remain in the
22 macrophages with an efficiency twenty times higher than that of its parent drug ($P < 0.001$). The
23 ability of UDCA-AZT to elude the AET systems (Dalpiaz et al., 2012), appears therefore useful in
24 order to induce its uptake in the macrophages. According to the data reported in Fig. 1 the presence
25 of the prodrug in the CSF should allow its permeation and permanence in the macrophages,
26 constituting therefore an efficient carrier for AZT.
27
28
29
30
31
32
33
34
35
36
37
38
39
40

41 *3.2. Characterization of microspheres*

42 *3.2.1. The yields of production*

43
44
45
46
47
48
49
50
51
52
53
54
55
56
57
58
59
60
61
62
63
64
65
66
67
68
69
70
71
72
73
74
75
76
77
78
79
80
81
82
83
84
85
86
87
88
89
90
91
92
93
94
95
96
97
98
99
100
101
102
103
104
105
106
107
108
109
110
111
112
113
114
115
116
117
118
119
120
121
122
123
124
125
126
127
128
129
130
131
132
133
134
135
136
137
138
139
140
141
142
143
144
145
146
147
148
149
150
151
152
153
154
155
156
157
158
159
160
161
162
163
164
165
166
167
168
169
170
171
172
173
174
175
176
177
178
179
180
181
182
183
184
185
186
187
188
189
190
191
192
193
194
195
196
197
198
199
200
201
202
203
204
205
206
207
208
209
210
211
212
213
214
215
216
217
218
219
220
221
222
223
224
225
226
227
228
229
230
231
232
233
234
235
236
237
238
239
240
241
242
243
244
245
246
247
248
249
250
251
252
253
254
255
256
257
258
259
260
261
262
263
264
265
266
267
268
269
270
271
272
273
274
275
276
277
278
279
280
281
282
283
284
285
286
287
288
289
290
291
292
293
294
295
296
297
298
299
300
301
302
303
304
305
306
307
308
309
310
311
312
313
314
315
316
317
318
319
320
321
322
323
324
325
326
327
328
329
330
331
332
333
334
335
336
337
338
339
340
341
342
343
344
345
346
347
348
349
350
351
352
353
354
355
356
357
358
359
360
361
362
363
364
365
366
367
368
369
370
371
372
373
374
375
376
377
378
379
380
381
382
383
384
385
386
387
388
389
390
391
392
393
394
395
396
397
398
399
400
401
402
403
404
405
406
407
408
409
410
411
412
413
414
415
416
417
418
419
420
421
422
423
424
425
426
427
428
429
430
431
432
433
434
435
436
437
438
439
440
441
442
443
444
445
446
447
448
449
450
451
452
453
454
455
456
457
458
459
460
461
462
463
464
465
466
467
468
469
470
471
472
473
474
475
476
477
478
479
480
481
482
483
484
485
486
487
488
489
490
491
492
493
494
495
496
497
498
499
500
501
502
503
504
505
506
507
508
509
510
511
512
513
514
515
516
517
518
519
520
521
522
523
524
525
526
527
528
529
530
531
532
533
534
535
536
537
538
539
540
541
542
543
544
545
546
547
548
549
550
551
552
553
554
555
556
557
558
559
560
561
562
563
564
565
566
567
568
569
570
571
572
573
574
575
576
577
578
579
580
581
582
583
584
585
586
587
588
589
590
591
592
593
594
595
596
597
598
599
600
601
602
603
604
605
606
607
608
609
610
611
612
613
614
615
616
617
618
619
620
621
622
623
624
625
626
627
628
629
630
631
632
633
634
635
636
637
638
639
640
641
642
643
644
645
646
647
648
649
650
651
652
653
654
655
656
657
658
659
660
661
662
663
664
665
666
667
668
669
670
671
672
673
674
675
676
677
678
679
680
681
682
683
684
685
686
687
688
689
690
691
692
693
694
695
696
697
698
699
700
701
702
703
704
705
706
707
708
709
710
711
712
713
714
715
716
717
718
719
720
721
722
723
724
725
726
727
728
729
730
731
732
733
734
735
736
737
738
739
740
741
742
743
744
745
746
747
748
749
750
751
752
753
754
755
756
757
758
759
760
761
762
763
764
765
766
767
768
769
770
771
772
773
774
775
776
777
778
779
780
781
782
783
784
785
786
787
788
789
790
791
792
793
794
795
796
797
798
799
800
801
802
803
804
805
806
807
808
809
810
811
812
813
814
815
816
817
818
819
820
821
822
823
824
825
826
827
828
829
830
831
832
833
834
835
836
837
838
839
840
841
842
843
844
845
846
847
848
849
850
851
852
853
854
855
856
857
858
859
860
861
862
863
864
865
866
867
868
869
870
871
872
873
874
875
876
877
878
879
880
881
882
883
884
885
886
887
888
889
890
891
892
893
894
895
896
897
898
899
900
901
902
903
904
905
906
907
908
909
910
911
912
913
914
915
916
917
918
919
920
921
922
923
924
925
926
927
928
929
930
931
932
933
934
935
936
937
938
939
940
941
942
943
944
945
946
947
948
949
950
951
952
953
954
955
956
957
958
959
960
961
962
963
964
965
966
967
968
969
970
971
972
973
974
975
976
977
978
979
980
981
982
983
984
985
986
987
988
989
990
991
992
993
994
995
996
997
998
999
1000

3.2.2. *UDCA-AZT content in CP*

The amount of encapsulated UDCA-AZT in CP sample was found to be $13 \pm 0.3\%$ (w/w),

1 showing that chitosan, characterized by hydrophilic properties, was able to encapsulate the
2 lipophilic prodrug with a good encapsulation efficiency ($64.9\pm 1.5\%$).
3
4
5
6

7 3.2.3. Particle size measurement

8
9 Table 1 reports the volume-surface diameters (d_{vs}) obtained for the loaded (CP) and unloaded
10 microparticles (CH), for MIX and, finally, for chitosan chloride and UDCA-AZT before and after
11 grinding by agate and mortar and pestle. The loading of UDCA-AZT into chitosan microparticles
12 determined an increase of particle size: in fact CP microspheres had d_{vs} of 3.59 ± 0.1 μm compared
13 with 2.32 ± 0.01 μm of CH ($P < 0.0001$). Furthermore, the drug presence resulted in a change of
14 particle size distribution: loaded microparticles showed a larger curve than that of drug free
15 microspheres (Fig. 2 up). In particular, CH showed a Gaussian curve while CP curve appeared
16 leptokurtic, right skewed and wide for the presence of small shoulders.
17
18
19
20
21
22
23
24
25
26
27
28

29 MIX had d_{vs} of 6.11 ± 0.022 μm , significantly higher than microspheres ($P < 0.001$) and UDCA-
30 AZT alone, but significant lower than chitosan chloride alone, both analyzed after grinding. The
31 grinding of drug and polymer in agate mortar determined a reduction of particles size and a shifting
32 of size distributions to low values (Fig. 2 down). In fact, the d_{vs} of chitosan chloride changed from
33 19.98 ± 0.24 μm to 12.67 ± 0.819 μm because of aggregates break. More pronounced was the size
34 reduction in case of UDCA-AZT crystals: the d_{vs} decreased from 23.33 ± 0.06 μm to 5.12 ± 0.018 μm
35 after grinding.
36
37
38
39
40
41
42
43
44
45
46
47

48 3.2.4. Particle morphology

49
50 Fig. 3A reports the SEM image of MIX obtained by geometric dilution with the use of agate
51 mortar and pestle. This picture evidenced not only particles characterized by round morphology and
52 relatively smooth surface, but also the presence of fragments characterized by irregular shape. As a
53 term of comparison, Figs 3B and 3C report the SEM images of chitosan chloride and UDCA-AZT,
54 respectively, grinded by agate mortar and pestle. Fig. 3B showed particles characterized by round
55
56
57
58
59
60
61
62
63
64
65

1 morphology and smooth surface. These morphologic characteristic did not appear significantly
2 different from those of chitosan chloride before grinding, as evidenced by its SEM image reported
3 in Fig. 3E. The SEM picture of grinded UDCA-AZT, Fig. 3C, showed fragments characterized by
4 irregular shape (a detail is evidenced in the SEM image reported in Fig. 3D) with high aptitude to
5 aggregate. These morphologic characteristic appeared significantly different from those of the
6 prodrug UDCA-AZT before grinding, as evidenced in Fig. 3F, where fragments of irregular shape
7 are shown to be characterized by diameters at least one order of magnitude higher than those of
8 grinded UDCA-AZT particles. Taking into account these aspects, we can conclude that the SEM
9 image of the physical mixture of chitosan chloride and UDCA-AZT (Fig. 3A) allows us to
10 discriminate its two components: in particular, the particles with round morphology can be
11 attributed to chitosan chloride, whereas the fragments of irregular shape can be attributed to UDCA-
12 AZT.

13
14
15
16
17
18
19
20
21
22
23
24
25
26
27
28
29 Fig. 4A and 4B report SEM images of CP, constituted by the loaded UDCA-AZT
30 microparticles based on chitosan chloride. The pictures evidence the presence of spherical particles
31 characterized by smooth surface and several fragments characterized by irregular shape and high
32 porosity, similar to spongy balls showing a some degree of aggregation. As a term of comparison,
33 Fig. 4C reports the SEM image of the unloaded microparticles (CH), evidencing their round shape
34 with smooth surfaces. Taking into account these aspects we can hypothesize that the spherical
35 particles evidenced in images 3A and 3B are constituted by unloaded chitosan chloride, whereas the
36 spongy balls have been obtained by the interaction between chitosan chloride and UDCA-AZT,
37 giving rise to the highly porous structures.

3.2.5. *True density*

38
39
40
41
42
43
44
45
46
47
48
49
50
51
52
53
54
55
56 True density of microspheres was $1.48 \pm 0.02 \text{ g/cm}^3$ that is comparable with ρ of nasal
57 microspheres (Gavini et al., 2012).
58
59
60
61
62
63
64
65

3.2.6. Determination of water uptake capacity

Fig. 5 shows the water uptake of both loaded and unloaded formulations. Free drug formulations absorbed a greater amount of water than loaded microparticles. Drug loading decreased the water absorption capability of chitosan microspheres ($P < 0.05$). UDCA–AZT and chitosan chloride physical mixture showed also water uptake capability larger than CP but lower than CH from 15 to 60 min ($P < 0.05$).

3.3. In-vitro release and dissolution studies

The dissolution and release studies of UDCA–AZT were performed in a MeOH/H₂O (70:30, v/v) mixture. The employment of methanol as cosolvent was necessary to increase the low solubility of the prodrug in water (0.0030 ± 0.0001 mg/ml; Dalpiaz et al., 2012), thus ensuring sink conditions.

Fig. 6 reports the release profile of UDCA–AZT from the loaded CP sample. The release pattern is compared with that of UDCA–AZT dissolution from its physical mixture with chitosan chloride. The dissolution rate of the prodrug included in MIX appeared significantly lower than that of UDCA–AZT loaded in the CP sample. Indeed, after two hours of incubation the $38.4 \pm 1.6\%$ of the prodrug loaded in the dissolution apparatus appeared dissolved, whereas in the case of CP loaded microparticles the amount of UDCA–AZT dissolved was $86.2 \pm 3.4\%$. As a consequence the dissolution half-life of UDCA–AZT loaded in CP sample appeared of about 15 min, whereas for the prodrug in the physical mixture (MIX) the dissolution half-life was higher than two hours. These profiles suggest that the employment of the CP sample as nasal formulation should be appropriate, being able to release in relatively short time the prodrug UDCA–AZT, allowing its potential fast absorption following the administration of the microparticles.

3.4. In-vivo UDCA-AZT administration

1
2 Taking into account that the CP microparticles were characterized not only by a satisfactory
3 encapsulation efficiency but also by their ability to induce a relatively fast dissolution of
4 UDCA–AZT, we have tested these microparticles for nasal administration of the prodrug, in order
5 to verify its potential uptake in the CNS. The nasal administration of UDCA–AZT was performed
6 with the employment of three different formulations: (i) a suspension in water of the raw UDCA-
7 AZT powder, (ii) the powder constituted by loaded CP microparticles and (iii) as term of
8 comparison, the parent physical mixture of chitosan chloride and UDCA-AZT (87:13 w/w). The
9 results have been compared with those obtained by the intravenous infusion of UDCA–AZT to rats.
10
11
12
13
14
15
16
17
18
19
20
21
22
23

24 3.4.1. Intravenous administration of UDCA–AZT

25
26 The prodrug was undetectable in rat blood samples following its intravenous infusion. This
27 result is in agreement with the very fast hydrolysis of UDCA–AZT in rat blood at 37 °C (Dalpiaz et
28 al., 2012). Important amounts of AZT were therefore detected following the intravenous
29 administration of the prodrug, as evidenced in Fig. 7. In particular, after infusion of 0.200 mg of
30 UDCA–AZT to rats, the AZT concentration in the bloodstream was 4.50 ± 0.31 µg/mL and
31 decreased during time with an apparent first order kinetic confirmed by the linearity of the
32 semilogarithmic plot reported in the inset of Fig. 8 ($n = 9$, $r = 0.990$, $P < 0.0001$), and a half-life of
33 60.4 ± 3.8 min. These data are in good agreement with those obtained by previous studies on *in-vivo*
34 UDCA-AZT pharmacokinetics (Dalpiaz et al., 2014). No AZT or UDCA–AZT amounts were
35 detected in the CSF within 180 min after intravenous administration of UDCA–AZT.
36
37
38
39
40
41
42
43
44
45
46
47
48
49
50
51
52

53 3.4.2. Nasal Administration of UDCA–AZT

54
55 The nasal administration of pure UDCA-AZT as water suspension did not allow to obtain
56 detectable amounts of AZT or prodrug in blood or in CSF, respectively, within 180 min after the
57 administration, as previously evidenced (Dalpiaz et al., 2014). On the contrary, the nasal
58
59
60
61
62
63
64
65

1 administration of the powders constituted by MIX or by the CP microparticles (0.8 mg, about 100
2 μg of UDCA–AZT to each nostril) produced detectable amounts of UDCA–AZT in the CSF of the
3 rats, as reported in Fig. 8. In particular, the UDCA–AZT concentrations in the CSF were 0.64 ± 0.12
4 $\mu\text{g}/\text{mL}$ and 1.96 ± 0.29 $\mu\text{g}/\text{mL}$ at 30 and 60 min after nasal administration of the mixture
5
6 respectively. The UDCA–AZT concentration then decreased, reaching the value of 0.60 $\mu\text{g}/\text{mL}$ at
7
8
9
10
11
12 180 min.

13
14 The nasal administration of the same amount of CP microparticles allowed to increase the rate
15 uptake of the prodrug in the CSF of rats. Indeed, the UDCA–AZT concentrations in the CSF were
16
17 2.30 ± 0.09 $\mu\text{g}/\text{mL}$ and 2.99 ± 0.31 $\mu\text{g}/\text{mL}$ at 30 and 60 min after nasal administration of the CP
18
19 sample, respectively. The UDCA–AZT concentration then decreased, reaching the value of 1.12
20
21 $\mu\text{g}/\text{mL}$ at 180 min. No AZT amounts were detected in the bloodstream and in CSF within 180 min
22
23 after nasal administration of the powders constituted by MIX or the CP microparticles.
24
25
26
27
28

29 The area under concentration (AUC) curve values obtained for UDCA–AZT in the CSF,
30 following the nasal administration of MIX and CP microparticles (Fig. 8), were 201.39 ± 13.51 μg
31
32 mL^{-1} min and 354.4 ± 13.3 $\mu\text{g mL}^{-1}$ min, respectively. The ratio between AUC of CP sample and
33
34 AUC of the mixture was 1.76, indicating that the nasal formulation constituted by CP
35
36 microparticles allowed an uptake of UDCA–AZT in the CSF the 76% higher than that obtained by
37
38 the administration of the parent mixture.
39
40
41
42
43
44
45

46 **4. Discussion**

47
48
49
50

51 Although antiretroviral nucleoside derivatives are largely used in AIDS treatment for their
52 efficacy at peripheral level, a total eradication of HIV from the body is currently hard to be
53
54 obtained. Indeed, the antiretroviral drugs are not able to reach the central nervous system (CNS),
55
56 (Kaufmann and Cooper, 2000; Strazielle, 2003) that is instead easily reached by HIV through
57
58 infected monocytes (Davis et al., 1992; Gray et al., 1996) that differentiate into macrophages and
59
60
61
62
63
64
65

1 microglia in the brain (Rausch and Stover, 2001). The CNS and the macrophages constitute,
2 therefore, sanctuaries of HIV, where drug resistance is induced and from which the periphery can
3 be reinfected (Cunningham et al., 2000; Kolson and Gonzalez-Scarano, 2000). These phenomena
4 are mainly attributed to the expression of active efflux transporters (AET) on the membranes of the
5 macrophages (Chaudhary et al., 1992; Neyfakh et al., 1989) and the blood brain barrier (BBB) cells
6 (Namanja et al., 2012; Pavan and Dalpiaz 2011), whose activity causes the lack of penetration of
7 antiretroviral drugs in the HIV sanctuaries.
8

9
10
11
12
13
14
15
16
17 The AZT activity in the CNS appears necessary not only in the brain tissue, but also in the CSF
18 subarachnoid spaces containing macrophages, that constitute the only site of HIV replication in the
19 brain (Gherzi-Egea et al., 1996; Cunningham et al., 1997). It should therefore be important to obtain
20 formulations able to target AZT in the CSF, but it should also as much important to induce its
21 ability to elude the AET systems, in order to avoid its extrusion from the CNS and from the
22 macrophages. In this regards we know that the prodrug UDCA-AZT, obtained by the conjugation of
23 AZT with the ursodeoxycholic acid (UDCA), is able to elude the AET systems (Dalpiaz et al.,
24 2012). Moreover, the results reported in this paper evidence for the first time that the prodrug
25 UDCA-AZT is definitely more efficient than AZT in permeating and remaining into murine
26 macrophage-like J774A.1 cell line, commonly used as model system for studying the internalization
27 process of macrophages (Wang et al., 2012). It is to remark that the prodrug UDCA-AZT is quickly
28 hydrolyzed in whole blood, so an intravenous administration cannot be suitable for its permeation
29 across the BBB. Indeed, following this type of administration we have detected only AZT amounts,
30 showing concentration values decreasing during time with a half-life of about 1 h. No AZT and
31 UDCA-AZT amounts were detected in the CSF of rats after intravenous administration. On the
32 other hand, the nasal administration of this prodrug appears promising in order to obtain its uptake
33 in the CNS and, in particular, in CSF. We have indeed demonstrated that the nasal administration of
34 chitosan based microparticles can induce a selective uptake of neuroactive agents in the CSF of rats,
35 probably by promoting drug permeation across olfactory nasal mucosa (Dalpiaz et al., 2008; Gavini
36
37
38
39
40
41
42
43
44
45
46
47
48
49
50
51
52
53
54
55
56
57
58
59
60
61
62
63
64
65

1 et al., 2011; Rassa et al., 2015a). Very recently, the poor water solubility of UDCA-AZT
2 encouraged us to encapsulate this prodrug in solid lipid microparticles (Dalpiaz et al., 2014). In
3 particular, the nasal administration of UDCA-AZT loaded in stearic acid based microparticles
4 induced a selective uptake of the prodrug in the CSF of rats, with amounts up to about 0.4 µg/ml
5 within 60 min after the administration (Dalpiaz et al., 2014). These amounts were sensibly
6 increased (up to about 1.50 µg/mL within 120 min after the administration) when the same quantity
7 of microparticles were nasally administered as a water suspension in the presence of chitosan
8 chloride (Dalpiaz et al., 2014). This result was attributed to the good mucoadhesive properties of
9 chitosan (Dalpiaz et al., 2008) and to its ability to transiently open the tight junctions in the
10 epithelial membranes (Illum et al., 1994; Dodane et al, 1999).
11
12
13
14
15
16
17
18
19
20
21
22
23

24 Nasal formulation obtained in the presence of water can be related to risk of chemical and
25 physical instability and microbiological growth. Moreover, in the nasal cavity the liquid
26 formulations are often rinsed into the gastrointestinal tract (GIT) or out, so their residence time is
27 generally short (Kublik and Vidgren, 1998). These disadvantages can be overcome by using
28 powder-based formulations (Marttin et al., 1997; Rassa et al., 2015b). For this reason we have
29 prepared microspheres based on chitosan chloride in order to increase the nose-to-brain delivery of
30 UDCA-AZT. The efficacy of the microparticulate system on the brain delivery of the prodrug was
31 verified by comparing the properties of microparticles with those of their parent physical mixture,
32 that was obtained by geometrical dilution of the components with the use of agate mortar and
33 pestle. The grinding process induced a decrease of the d_{vs} diameters of chitosan chloride and
34 UDCA-AZT particles. The chitosan chloride particles were characterized by round morphology
35 and a relatively smooth surface before and after grinding, whereas UDCA-AZT appeared as
36 fragments with irregular shape. These two different morphological characteristics were distinctly
37 recognized in the SEM picture of the physical mixture, where small irregular fragments of UDCA-
38 AZT appeared on the surface of larger and round chitosan chloride microspheres.
39
40
41
42
43
44
45
46
47
48
49
50
51
52
53
54
55
56
57
58
59
60
61
62
63
64
65

1 The spray-drying process allowed to obtain unloaded microparticles of chitosan chloride (CH)
2 with the “classical” round morphology and small d_{vs} diameter. The loaded microparticles (CP)
3 evidenced a slight increase of size and a morphology characterized by spherical particles mixed
4 with fragments of irregular shape and high porosity, similar to spongy balls showing a some degree
5 of aggregation. It can be deduced that the spherical particles are attributable to pure chitosan
6 chloride, that during the spray drying process has not interacted with UDCA-AZT, whereas the
7 “spongy balls” were obtained by a combination of the prodrug with polymer, inducing the
8 formation of the highly porous structures. The totally different degree of water solubility between
9 UDCA-AZT and chitosan can justify these characteristics of the CP formulation. The description
10 of CP’s morphology appears in agreement with the dissolution and water uptake profiles. Indeed,
11 we have observed that the dissolution rate of UDCA-AZT from the CP sample was sensibly higher
12 than that from the parent physical mixture. This phenomenon can be attributable to the highly
13 porous structures observed in CP sample, that allows a faster dissolution of UDCA-AZT with
14 respect to its fragments included in MIX. Moreover, as previously demonstrated by Gavini et al.,
15 2011, water soluble chitosans, such as salts, are more able to completely amorphize poorly soluble
16 drugs into the polymer matrix compared to chitosan base; as consequence, the improvement of the
17 dissolution rate of poorly soluble drugs and their bioavailability occur.

18
19 Moreover, we have observed that the water uptake rate of CH sample was significantly
20 reduced if chitosan chloride was mixed with UDCA-AZT, but a drastic decrease was observed in
21 the case of CP sample. The presence of UDCA-AZT, a very poor water soluble molecule, in the
22 physical mixture can explain its reduction of water uptake with respect to the CH sample, but the
23 drastic reduction registered for CP microparticles can be attributed to their porous structures, where
24 the presence of the prodrug and chitosan chloride together contributed to dramatically reduce the
25 water uptake aptitude of the polymer.

26
27 The CP sample appeared therefore as a valuable formulation for the nasal administration of
28 UDCA-AZT: in particular, we have hypothesized that the size and density of the microparticles

1 should induce their deposition on nasal mucosa, that should not be dehydrated by their presence,
2 being poor the water uptake of this sample. Moreover, the ability of the loaded microparticles to
3 increase the dissolution rate of UDCA-AZT suggested their potential aptitude to induce the prodrug
4 permeation across nasal mucosa, a phenomenon probably potentiated by the chitosan ability to
5 transiently open their tight junctions (Illum et al., 2015).
6
7
8
9
10

11 The nasal administration to rats of raw UDCA–AZT did not produced any detectable levels of
12 both UDCA–AZT and AZT in the bloodstream and CSF, whereas the nasal administration of the
13 CP sample and its parent physical mixture allowed to obtain relatively high levels of UDCA-AZT
14 in the CSF of rats, 60 min after their administration. The relative bioavailability attributed to the CP
15 sample was the 176% with respect to its parent physical mixture ($P < 0.001$). No AZT amount were
16 detected in the bloodstream of rats after nasal administration of CP sample and its parent physical
17 mixture, confirming the existence of a direct nose–CNS pathway for this prodrug (Dalpiaz et al.,
18 2014). Our results evidence that the role of chitosan in inducing the selective UDCA-AZT uptake
19 in the CSF is potentiated when formulated as microparticulate system by spray-drying. This
20 phenomenon appears clearly illustrated in Fig. 9, reporting a comparison of the AUC values in CSF
21 obtained after the nasal administration to rats of the same dose of UDCA-AZT (200 μg) by using
22 different formulations, i.e. the solid lipid microparticles (SLMs), their water dispersion in the
23 presence of chitosan (SLMs + Ch), previously obtained by Dalpiaz et al., 2014, MIX and CP, here
24 described. In particular CP was able to induce an uptake of UDCA-AZT in the CSF of rats 1.8, 3.2
25 and 18.6 times higher than its parent physical mixture (MIX), the dispersion of solid lipid particles
26 in the presence of chitosan (SLMs + Ch) and the SLMs in the solid form, respectively.
27
28
29
30
31
32
33
34
35
36
37
38
39
40
41
42
43
44
45
46
47
48
49
50

51 In conclusion, chitosan microspheres induce, after nasal administration, an efficient uptake of
52 UDCA-AZT in the CSF; thus, the ability of the prodrug to elude the AET systems can avoid its
53 extrusion in the bloodstream and induce the AZT transport in the macrophages located in the
54 subarachnoid spaces of CSF.
55
56
57
58
59
60
61
62
63
64
65

Acknowledgements

This research was supported by a grant from Ministero dell'Istruzione, dell'Università e della Ricerca (PRIN 2012).

References

- Bernkop-Schnürch, A., Dünnhaupt, S., 2012. Chitosan-based drug delivery systems, *Eur. J. Pharm. Biopharm.* 81, 463-469.
- Casettari, L., Illum, L., 2014. Chitosan in nasal delivery systems for therapeutic drugs. *J. Control. Rel.* 190:189-200.
- Chaudhary, P.M., Mechetner, E.B., Roninson, I.B., 1992. Expression and activity of the multidrug resistance p-glycoprotein in human peripheral blood lymphocytes. *Blood* 80, 2735–2739.
- Cho, W., Kim, M.S., Jung, M.S., Park, J., Cha, K.H., Kim, J.S., Park, H.J., Alhalaweh, A., Velaga, S.P., Hwang, S.J., 2014. Design of salmon calcitonin particles for nasal delivery using spray-drying and novel supercritical fluid-assisted spray-drying processes. *Int. J. Pharm.* 478, 288-296.
- Cunningham, A. L., Naif, H., Saksena, N., Lynch, G., Chang, J., Li, S., Jozwiak, R., Alali, M., Wang, B., Fear, W., Sloane, A., Pemberton, L., Brew, B., 1997. HIV infection of macrophages and pathogenesis of AIDS dementia complex: interaction of the host cell and viral genotype. *J. Leukocyte Biol.* 62, 117–125.
- Cunningham, P.H., Smith, D.G., Satchell, C., Cooper, D.A., Brew, B., 2000. Evidence for independent development of resistance to HIV-1 reverse transcriptase inhibitors in the cerebrospinal fluid. *AIDS* 14, 1949–1954.
- Dalpiaz, A., Gavini, E., Colombo, G., Russo, P., Bortolotti, F., Ferraro, L., Tanganelli, S., Scatturin, A., Menegatti, E., Giunchedi, P., 2008. Brain uptake of an antiischemic agent by nasal administration of microparticles. *J. Pharm. Sci.* 97, 4889–4903.

- 1 Dalpiaz, A., Paganetto, G., Pavan, B., Fogagnolo, M., Medici, A., Beggiato, S., Perrone, D., 2012.
2 Zidovudine and ursodeoxycholic acid conjugation: design of a new prodrug potentially able to
3 bypass the active efflux transport systems of the central nervous system. *Mol. Pharm.* 9,
4 957–968.
5
6
7
8
9 Dalpiaz, A., Ferraro, L., Perrone, D., Leo, E., Iannuccelli, V., Pavan, B., Paganetto, G., Beggiato,
10 S., Scalia, S., 2014. Brain uptake of a zidovudine prodrug after nasal administration of solid
11 lipid microparticles. *Mol. Pharm.*;11:1550-1561.
12
13
14
15
16
17 Davis, L.E., Hjelle, B.L., Miller, V.E., Palmer, D.L., Llewellyn, A.L., Merlin, T.L., Young, S.A.,
18 Mills, R.G., Wachsman, W., Wiley, C.A., 1992. Early viral brain invasion in iatrogenic
19 human immunodeficiency virus infection. *Neurology* 42, 1736–1739.
20
21
22
23
24 De Clercq, E., 2009. Anti-HIV Drugs: 25 compounds approved within 25 years after the discovery
25 of HIV. *Int. J. Antimicrob. Agents* 33, 307–320.
26
27
28
29 Dodane, V., Khan, M.A., Merwin, J.R., 1999. Effect of chitosan on epithelial permeability and
30 structure. *Int. J. Pharm.* 182, 21–32.
31
32
33
34 Fine, J.M., Forsberg, A.C., Renner, D.B., Faltsek. K.A., Mohan, K.G., Wong, J.C., Arneson, L.C.,
35 Crow, J.M., Frey. W.H. 2nd, Hanson. L.R., 2014. Intranasally-administered deferoxamine
36 mitigates toxicity of 6-OHDA in a rat model of Parkinson's disease. *Brain Res.* 1574, 96-104.
37
38
39
40
41 Fine, J.M., Renner, D.B., Forsberg, A.C., Cameron, R.A., Galick, B.T., Le, C., Conway, P.M.,
42 Stroebel, B.M., Frey, W.H. 2nd, Hanson, L.R., 2015. Intranasal deferoxamine engages
43 multiple pathways to decrease memory loss in the APP/PS1 model of amyloid accumulation.
44 *Neurosci. Lett.* 584, 362-367.
45
46
47
48
49
50
51 Finger, T.E., Jeor St., V.L., Kinnamon, J.C., Silver, W.L., 1990. Ultrastructure of substance P- and
52 CGRP-immunoreactive nerve fibers in the nasal epithelium of rodents. *J. Comp. Neurol.* 294,
53 293-305.
54
55
56
57
58
59
60
61
62
63
64
65

- 1
2
3
4
5
6
7
8
9
10
11
12
13
14
15
16
17
18
19
20
21
22
23
24
25
26
27
28
29
30
31
32
33
34
35
36
37
38
39
40
41
42
43
44
45
46
47
48
49
50
51
52
53
54
55
56
57
58
59
60
61
62
63
64
65
- Gavini, E., Rassu, G., Ferraro, L., Generosi, A., Rau, J.V., Brunetti, A., Giunchedi, P., Dalpiaz, A., 2011. Influence of chitosan glutamate on the in vivo intranasal absorption of rokitamycin from microspheres. *J. Pharm. Sci.* 100, 1488-1502.
- Gavini, E., Rassu, G., Ciarnelli, V., Spada, G., Cossu, M., Giunchedi, P., 2012. Mucoadhesive drug delivery systems for nose-to-brain targeting of dopamine. *J. Nanoneurosci.* 2, 47-55.
- Ghersi-Egea, J. F., Finnegan, W., Chen, J. L., Fenstermacher, J. D., 1996. Rapid distribution of intraventricularly administered sucrose into cerebrospinal fluid cisterns via subarachnoid velae in rat. *Neuroscience* 75, 1271–1288.
- Gray, F., Scaravilli, F., Everall, I., Chretien, F., An, S., Boche, D., Adle-Biassette, H., Wingertsman, L., Durigon, M., Hurtrel, B., Chiodi, F., Bell, J., Lantos, P., 1996. Neuropathology of early HIV-1 infection. *Brain Pathol.* 6, 1–15.
- Horvát, S., Fehér, A., Wolburg, H., Sipos, P., Veszeka, S., Tóth, A.; Kis, L., Kurunczi, A., Balogh, G., Kürti, L., Eros, I., Szabó-Révész, P., Deli, M. A., 2009. Sodium hyaluronate as a mucoadhesive component in nasal formulation enhances delivery of molecules to brain tissue. *Eur. J. Pharm. Biopharm* 72, 252–259.
- Illum, L., Farraj, N.F., Davis, S.S., 1994. Chitosan as a novel nasal delivery system for peptide drugs. *Pharm. Res.* 11, 1186–1189.
- Illum, L., 2000. Transport of drugs from the nasal cavity to the central nervous system. *Eur. J. Pharm. Sci.* 11, 1–18.
- Illum, L., 2004. Is nose-to-brain transport of drugs in man a reality? *J. Pharm. Pharmacol.*, 56, 3–17.
- Johnson, NJ., Hanson, L.R., Frey, W.H., 2010. Trigeminal pathways deliver a low molecular weight drug from the nose to the brain and orofacial structures. *Mol. Pharm.* 7, 884–893.
- Kaufmann, G.R., Cooper, D.A., 2000. Antiretroviral therapy of HIV-1 infection: established treatment strategies and new therapeutic options. *Curr. Opin. Microbiol.* 3, 508–514.
- Kolson, D.L., Gonzalez-Scarano, F., 2000. HIV and HIV dementia. *J. Clin. Invest.* 106, 11–13.

- 1
2
3
4
5
6
7
8
9
10
11
12
13
14
15
16
17
18
19
20
21
22
23
24
25
26
27
28
29
30
31
32
33
34
35
36
37
38
39
40
41
42
43
44
45
46
47
48
49
50
51
52
53
54
55
56
57
58
59
60
61
62
63
64
65
- Kublik, H., Vidgren, M.T., 1998. Nasal delivery systems and their effect on deposition and absorption, *Adv. Drug Del. Rev.* 29, 157–177.
- Maestrelli, F., Zerrouk, N., Chemtob, C., Mura, P., 2004. Influence of chitosan and its glutamate and hydrochloride salts on naproxen dissolution rate and permeation across Caco-2 cells. *Int. J. Pharm.* 271, 257-267.
- Marttin, E., Romeijn, S.G., Verhoef, J.C., Merkus, F.W.H.M., 1997. Nasal absorption of dihydroergotamine from liquid and powder formulations in rabbits, *J. Pharm. Sci.* 86, 802–807.
- Mistry, A., Stolnik, S., Illum, L., 2009. Nanoparticles for Direct nose to-brain delivery of drugs. *Int. J. Pharm.* 379, 146–157.
- Namanja, H.A.; Emmert, D.; Davis, D.A.; Campos, C.; Miller, D.S., Hrycyna, C.A., Chmielewski, J., 2012. Toward eradicating HIV reservoirs in the brain: inhibiting P-glycoprotein at the blood-brain barrier with prodrug abacavir dimers. *J. Am. Chem. Soc.* 134, 2976–2980.
- Neyfakh, A.A., Serpinskaya, A.S., Chervonsky, A.V., Apasov, S.G., Kazarov, A.R., 1989. Multidrug-resistance phenotype of a subpopulation of T-lymphocytes without drug selection. *Exp. Cell Res.* 185, 496–505.
- Pavan, B., Dalpiaz, A., 2011. Prodrugs and endogenous transporters: are they suitable tools for drug targeting into the central nervous system? *Curr. Pharm. Des.* 17, 3560–3535.
- Rassu, G., Gavini, E., Jonassen, H., Zambito, Y., Fogli, S., Breschi, M.C., Giunchedi, P., 2009. New chitosan derivatives for the preparation of rokitamycin loaded microspheres designed for ocular or nasal administration. *J. Pharm. Sci.* 98, 4852-4865.
- Rassu, G., Nieddu, M., Bosi, P., Trevisi, P., Colombo, M., Priori, D., Manconi, P., Giunchedi, P., Gavini, E., Boatto, G., 2014. Encapsulation and modified-release of thymol from oral microparticles as adjuvant or substitute to current medications. *Phytomedicine*, 21, 1627–1632.

- 1
2
3
4
5
6
7
8
9
10
11
12
13
14
15
16
17
18
19
20
21
22
23
24
25
26
27
28
29
30
31
32
33
34
35
36
37
38
39
40
41
42
43
44
45
46
47
48
49
50
51
52
53
54
55
56
57
58
59
60
61
62
63
64
65
- Rassu, G., Soddu, E., Cossu, M., Brundu, A., Cerri, G., Marchetti, N., Ferraro, L., Regan, R.F., Giunchedi, P., Gavini, E., Dalpiaz, A., 2015a. Solid microparticles based on chitosan or methyl- β -cyclodextrin: a first formulative approach to increase the nose-to-brain transport of deferoxamine mesylate. *J. Contr. Rel.* 201, 68–77.
- Rassu, G., Soddu, E., Cossu, M., Gavini, E., Giunchedi, P., Dalpiaz, A., 2015b. Powder formulations based on chitosan for nose-to-brain delivery of drugs, JDDST, in press, doi:10.1016/j.jddst.2015.05.002.
- Rausch, D.M., Stover, E.S., 2001 Neuroscience research in AIDS. *Prog. Neuropsychopharmacol. Biol. Psychiatry* 25, 231–257.
- Sacchetti, C., Artusi, M., Santi, P., Colombo, P., 2002. Caffeine microparticles for nasal administration obtained by spray drying. *Int. J. Pharm.* 242, 335–339.
- Sinha, V.R., Singla, A.K., Wadhawan, S., Kaushik, R., Kumria, R., Bansal, K., Dhawan, S., 2004. Chitosan microspheres as a potential carrier for drugs. *Int. J. Pharm.* 274, 1-33.
- Strazielle, N., Belin, M.F., Ghersi-Egea, J.F., 2003. Choroid plexus controls brain availability of anti-HIV nucleoside analogues via pharmacologically inhibitable organic anion transporters. *AIDS* 17, 1473–1485.
- Thorne, R.G., Frey, W.H., 2001. Delivery of neurotropic factors to the central nervous system. *Clin. Pharmacokinet.* 40, 907–946.
- Van den Berg, M. P., Romeijn, S. G., Verhoef, J. C., Merkus, F. W., 2002. Serial cerebrospinal fluid sampling in a rat model to study drug uptake from the nasal cavity. *J. Neurosci. Methods* 2002, 116, 99–107.
- Vyas, T.K., Shahiwala, A., Marathe, S., Misra, A., 2005. Intranasal drug delivery for brain targeting. *Curr. Drug Del.* 2, 165–175.
- Wang, Y., Sawchuk, R.J., 1995. Zidovudine transport in the rabbit during intravenous and intracerebroventricular infusion. *J. Pharm. Sci.* 7, 871–876.

1 Wang, H., Wu, L., Reinhard, B.M., 2012. Scavenger receptor mediated endocytosis of silver
2 nanoparticles into J774A.1 macrophages is heterogeneous. ACS Nano. 6(8), 7122-7132.
3
4
5
6
7
8
9
10
11
12
13
14
15
16
17
18
19
20
21
22
23
24
25
26
27
28
29
30
31
32
33
34
35
36
37
38
39
40
41
42
43
44
45
46
47
48
49
50
51
52
53
54
55
56
57
58
59
60
61
62
63
64
65

Caption of Figures

Fig. 1. Intracellular levels of AZT and its prodrug UDCA-AZT after incubation (30 min) with J774A.1 murine macrophages. Data are reported as the mean \pm S.D. of three independent experiments. *: $P < 0.001$ versus AZT.

Fig. 2. Size distribution of loaded (CP) and unloaded (CH) chitosan microspheres (up) as well as of MIX and, as comparison, of chitosan chloride and UDCA-AZT alone, before and after grinding (down). Particle size distribution was graphically expressed as curves obtained by plotting the volume of particles in percentage *versus* size (μm), shown in logarithmic scale

Fig. 3. Scanning electron microscopy (SEM) micrographs of [A] the mixture of chitosan chloride and UDCA-AZT (87:13 w/w, magnification of 3,610 times); [B] grinded chitosan chloride magnification of 3,140 times); grinded UDCA-AZT with magnification of 512 times [C] and 10,000 times [D]; [E] chitosan chloride before grinding (magnification of 2,740 times); [F] UDCA-AZT before grinding (magnification of 505 times).

Fig. 4. Scanning electron microscopy (SEM) micrographs with magnifications of 11,250 times [A] and 3,620 times [B] of the loaded microparticles (sample CP) and [C] SEM micrograph of unloaded chitosan microparticles (sample CH) with magnification of 2,000 times.

Fig. 5. Water Uptake profiles of loaded (CP) and unloaded (CH) microspheres until 60 min compared with that of physical mixture (MIX, chitosan chloride and UDCA-AZT (87:13 w/w). Data are reported as the mean \pm SD of three independent experiments.

Fig. 6. *In-vitro* release of UDCA-AZT from CP microparticles based on chitosan chloride. The

1
2
3
4
5
6
7
8
9
10
11
12
13
14
15
16
17
18
19
20
21
22
23
24
25
26
27
28
29
30
31
32
33
34
35
36
37
38
39
40
41
42
43
44
45
46
47
48
49
50
51
52
53
54
55
56
57
58
59
60
61
62
63
64
65

release profile is compared with that of dissolution obtained by the parent physical mixture of chitosan chloride and UDCA-AZT (87:13 w/w) (MIX). Data are reported as the mean±SD of three independent experiments.

Fig. 7. Elimination profile of AZT after 0.200 mg infusion of UDCA–AZT to rats. Data are expressed as the mean±SD of four independent experiments. The elimination followed an apparent first order kinetic, confirmed by the semilogarithmic plot reported in the inset (n =9, r = 0.990, P<0.0001). The half-life of AZT was calculated to be 60.4 ± 3.8 min.

Fig. 8. UDCA–AZT concentrations (µg/mL) detected in the CSF after nasal administration of loaded CP microparticles and its parent mixture (MIX) of chitosan chloride and UDCA-AZT. Each dose contained 200 µg of the prodrug. Data are expressed as the mean±SD of four independent experiments.

Fig. 9. A comparison among the AUC values obtained in CSF of rats after the nasal administration of 200 µg of UDCA-AZT by using different formulations, i.e. loaded solid lipid microparticles (SLMs), their water dispersion in the presence of chitosan (SLMs + Ch), the physical mixture of chitosan and prodrug (MIX) and the loaded microparticles based on chitosan chloride (CP). Data referred to SLMs and SLMs + Ch formulations were previously reported (Dalpiaz et al., 2014). Data are expressed as the mean±SD of four independent experiments.

Table 1.

Volume-surface diameters (d_{vs} , μm) of unloaded (CH) and loaded (CP) microparticles together with d_{vs} values of the parent mixture (MIX) of chitosan chloride and UDA-AZT and its single components before and after grinding by agate mortar and pestle. Data are reported as the mean \pm SD of three independent experiments.

Sample	d_{vs} (μm)
CP	3.59 ± 0.14
CH	2.32 ± 0.11
MIX	6.11 ± 0.02
Grinded Chitosan HCl	12.67 ± 0.82
Grinded UDCA-AZT	5.12 ± 0.02
Chitosan chloride before grinding	19.98 ± 0.06
UDCA-AZT before grinding	23.33 ± 0.06

Figure 1
[Click here to download high resolution image](#)

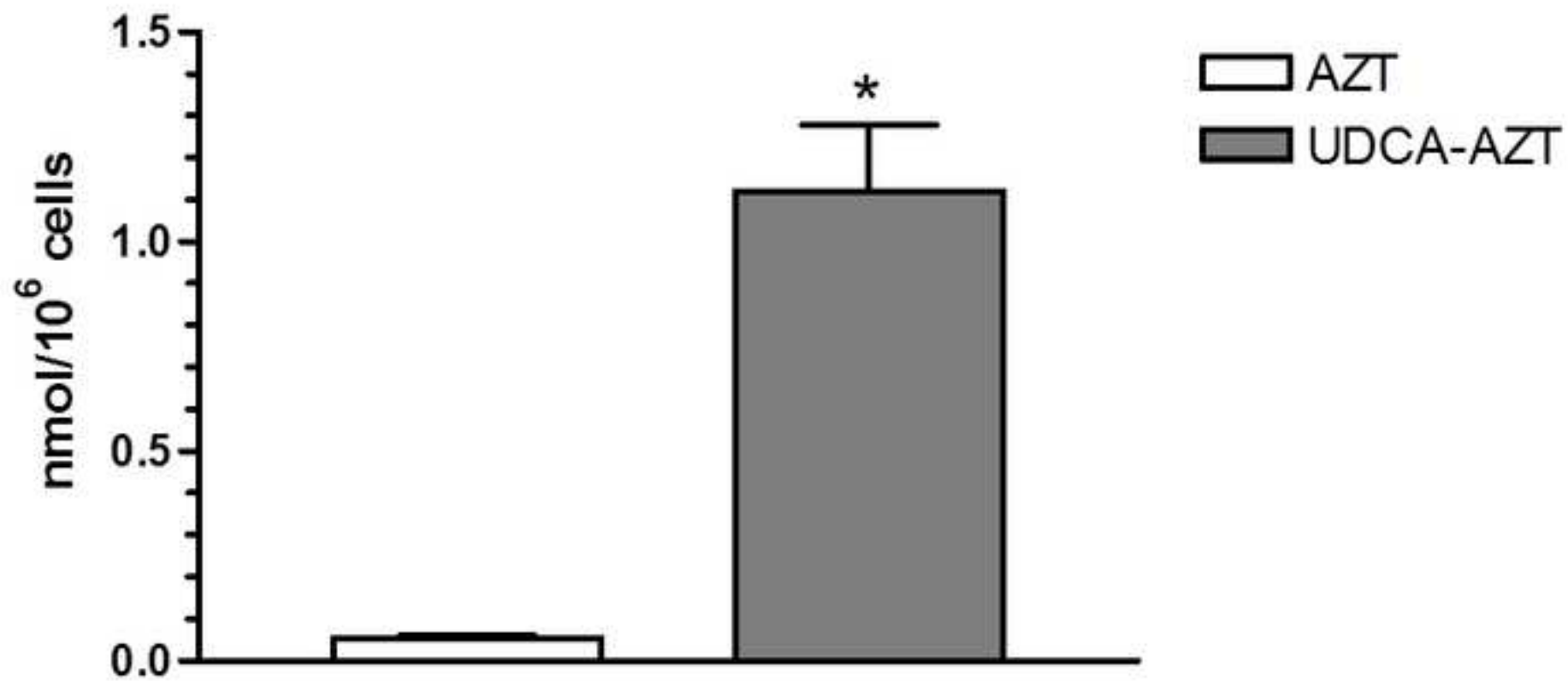


Figure 2

[Click here to download high resolution image](#)

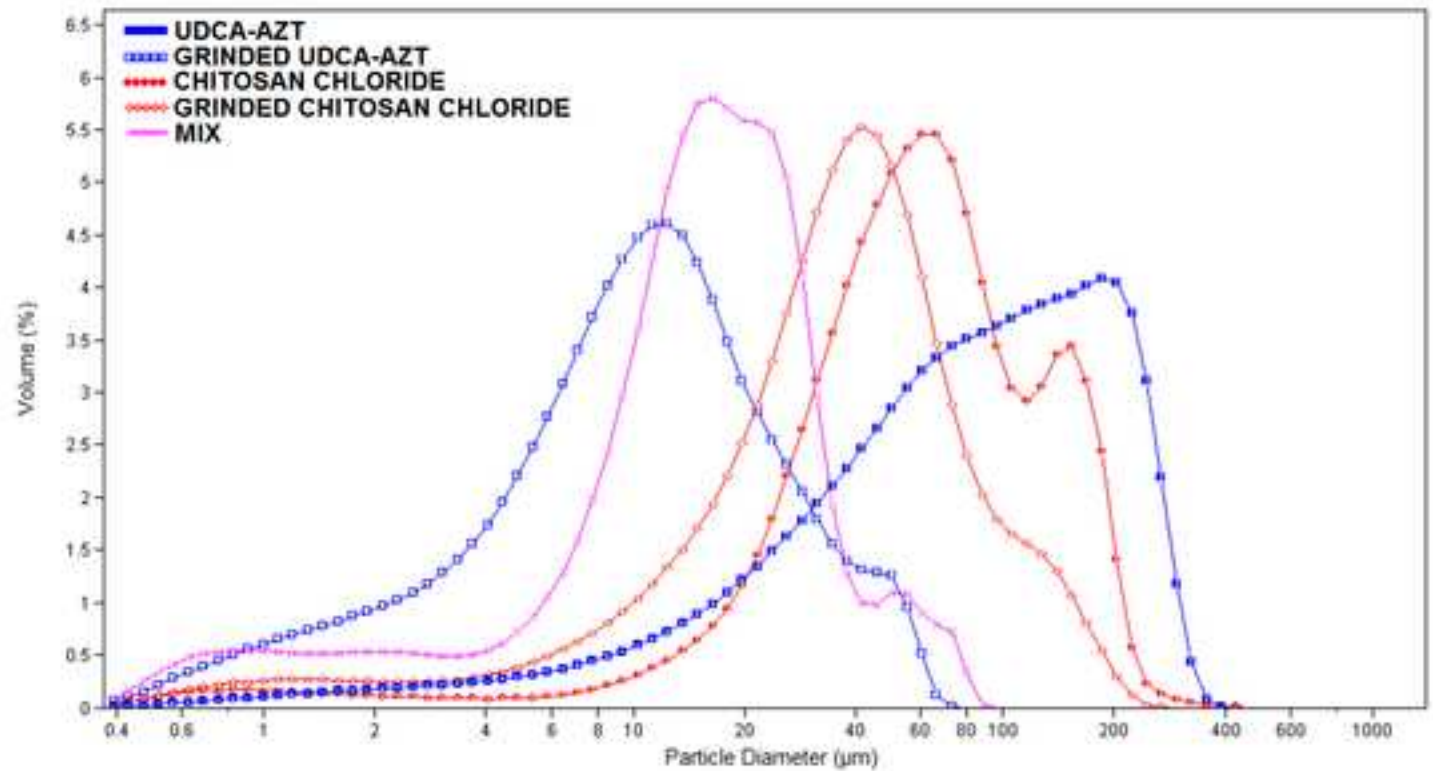
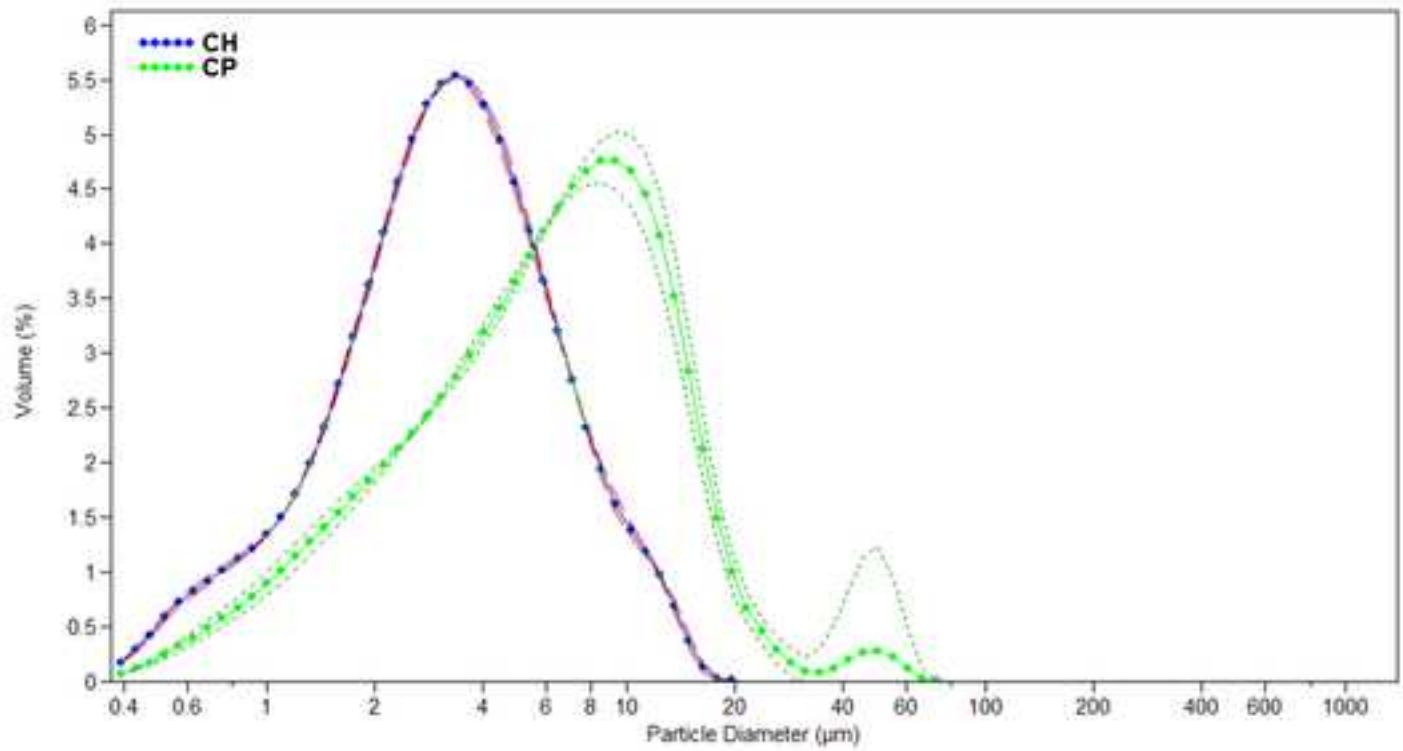


Figure 3
[Click here to download high resolution image](#)

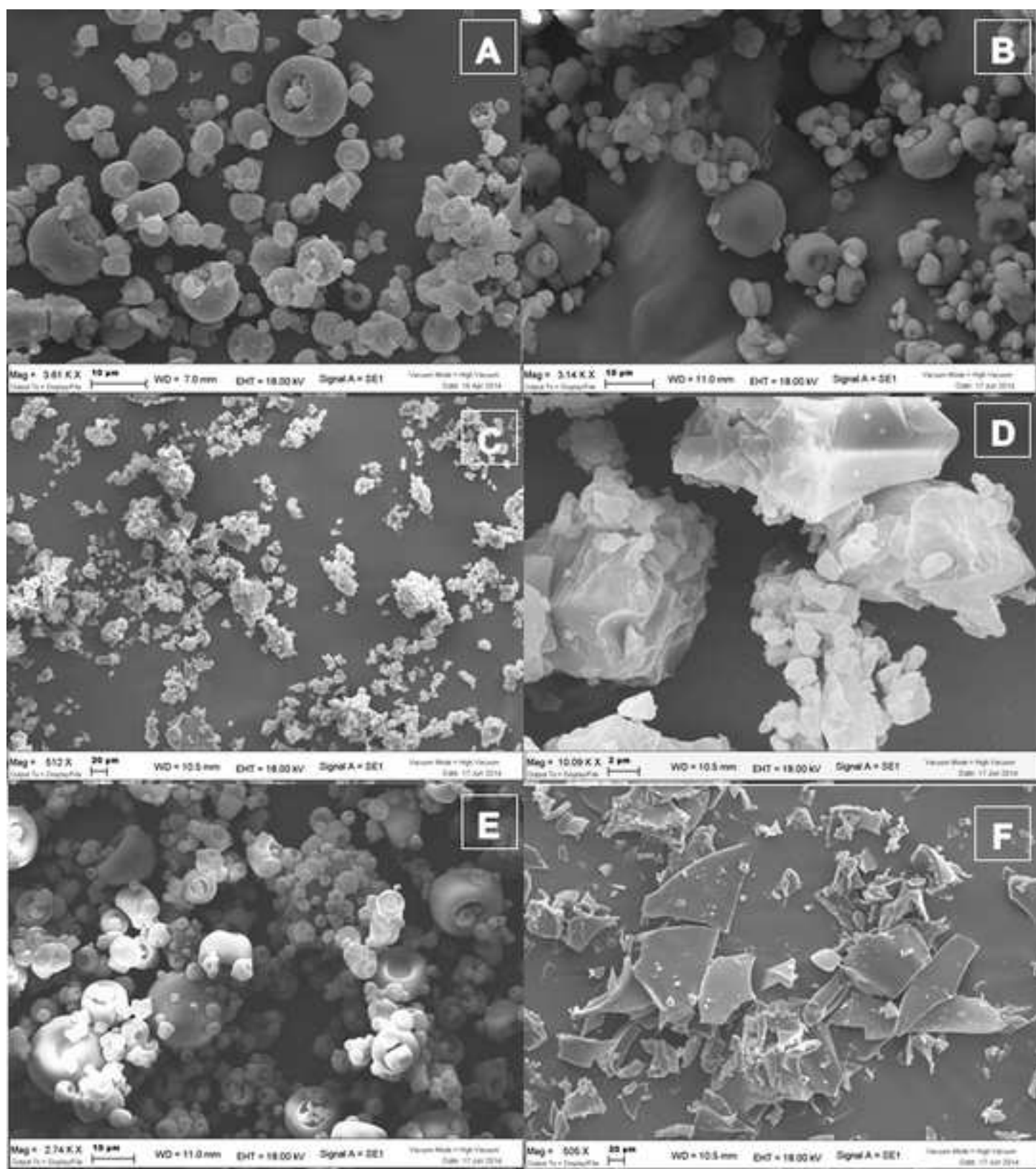


Figure 4
[Click here to download high resolution image](#)

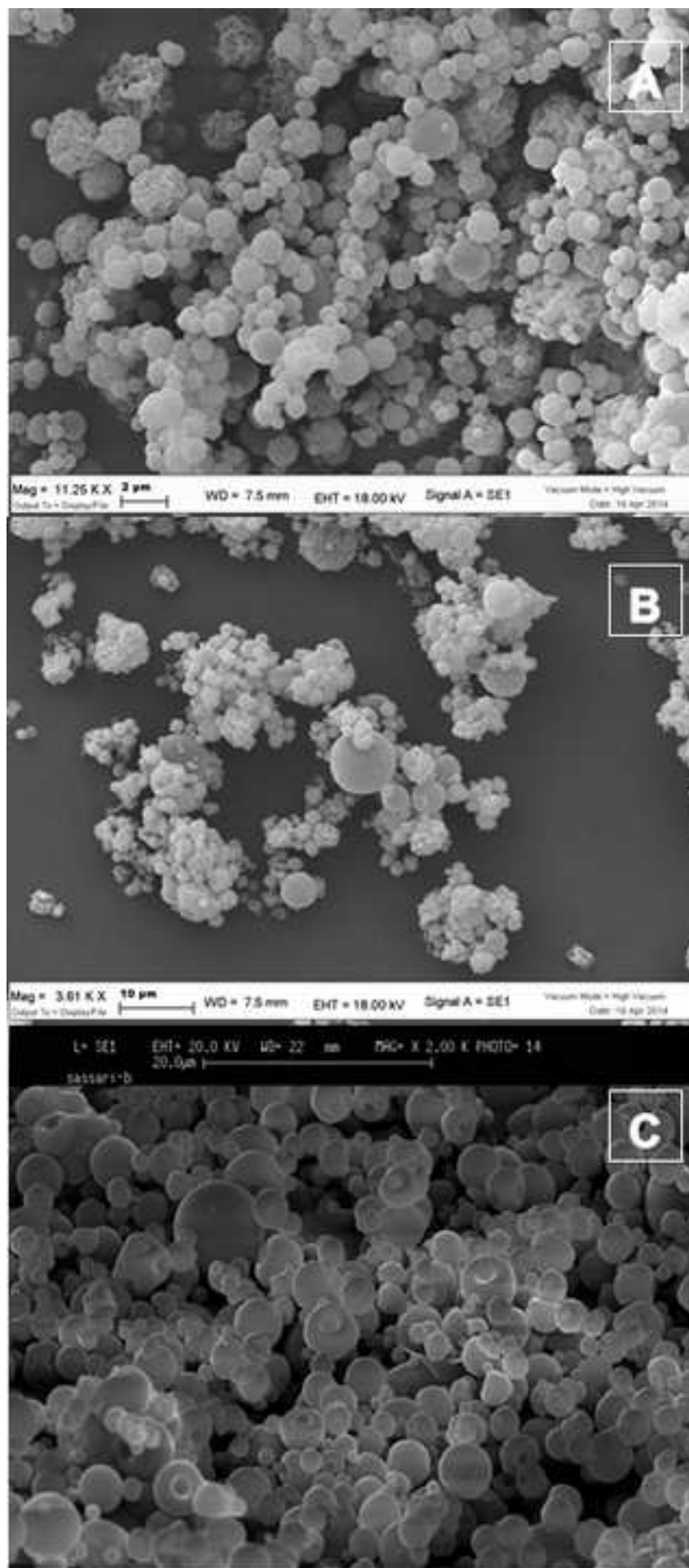


Figure 5
[Click here to download high resolution image](#)

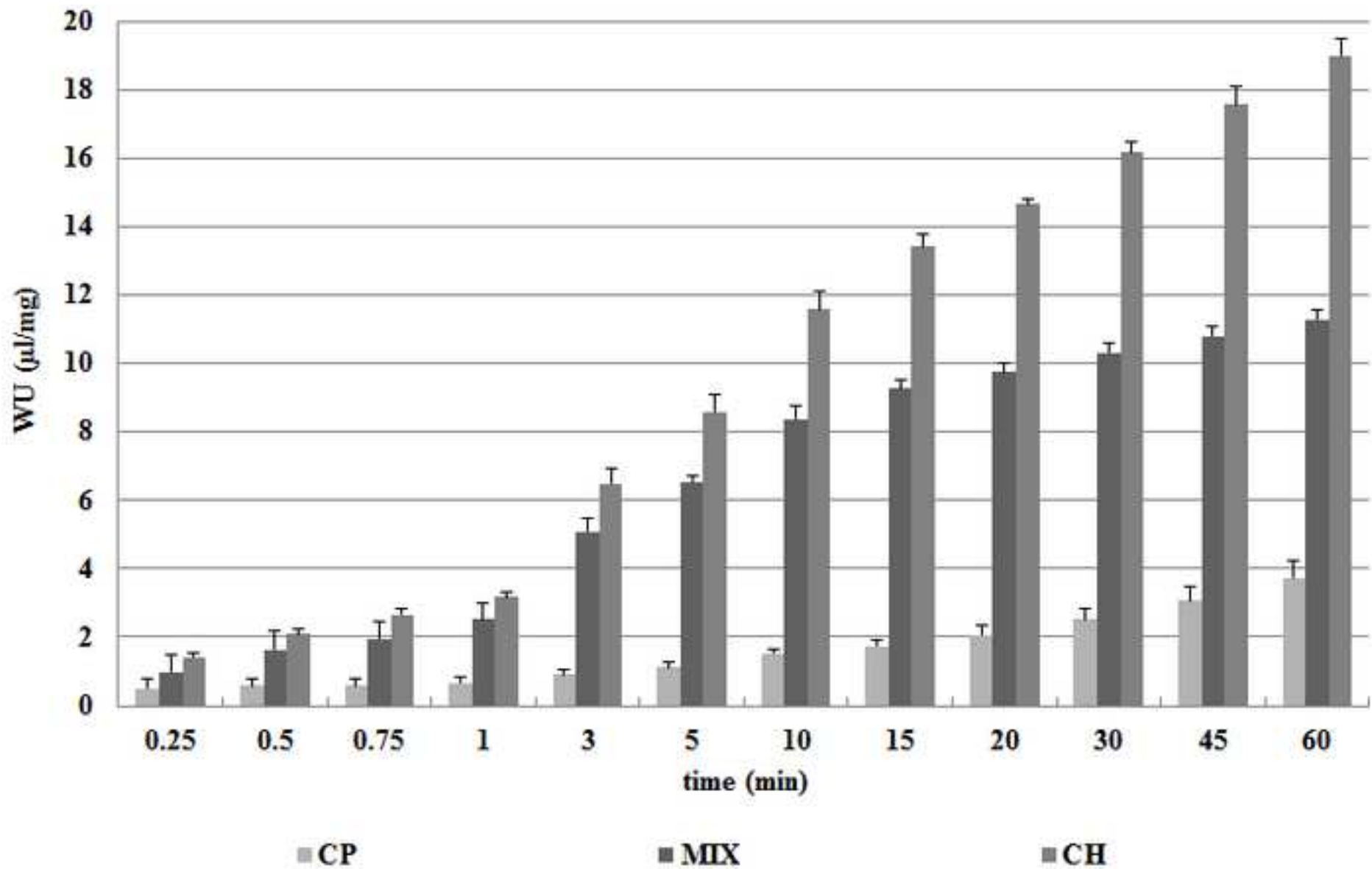


Figure 6
[Click here to download high resolution image](#)

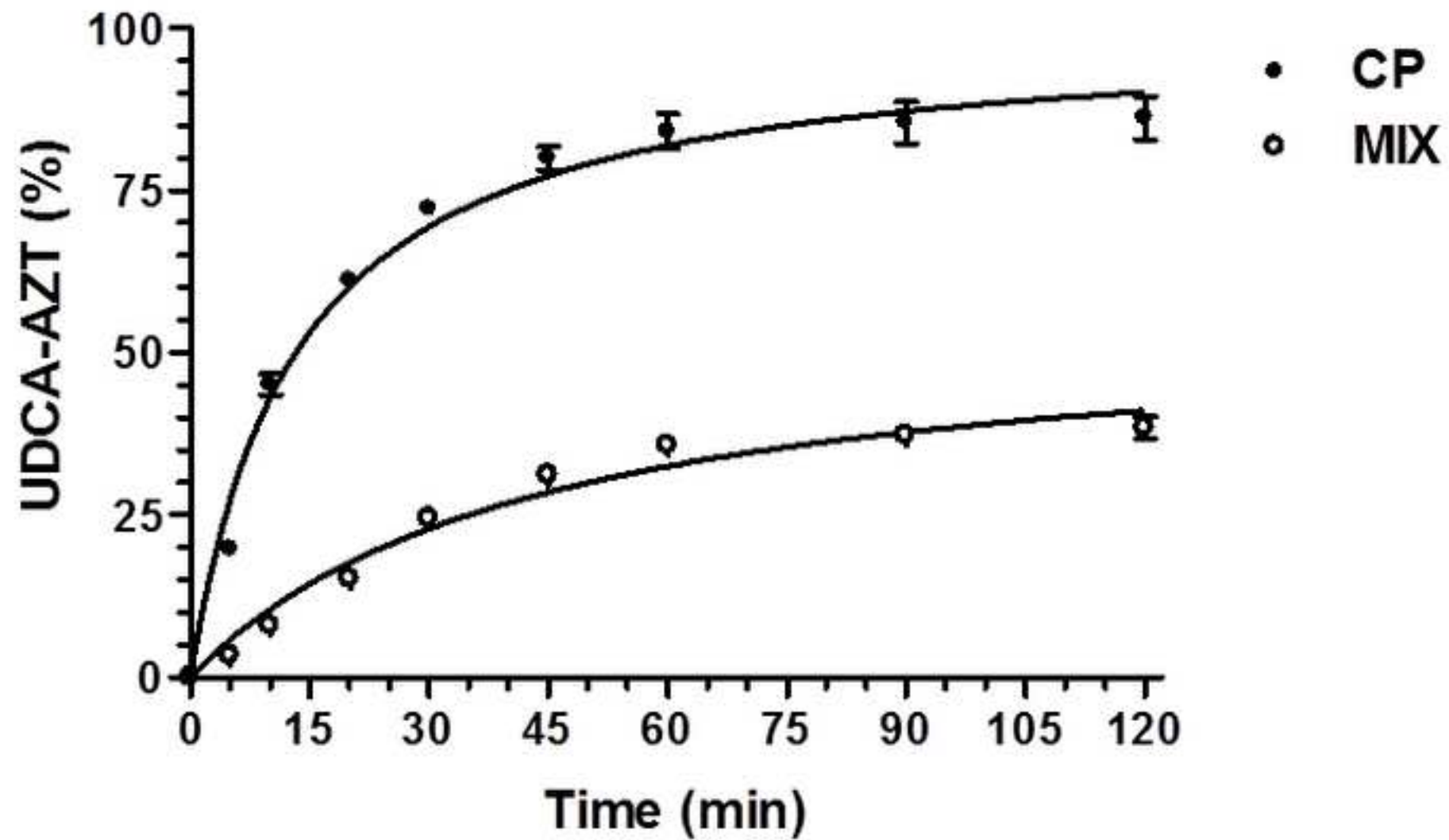


Figure 7
[Click here to download high resolution image](#)

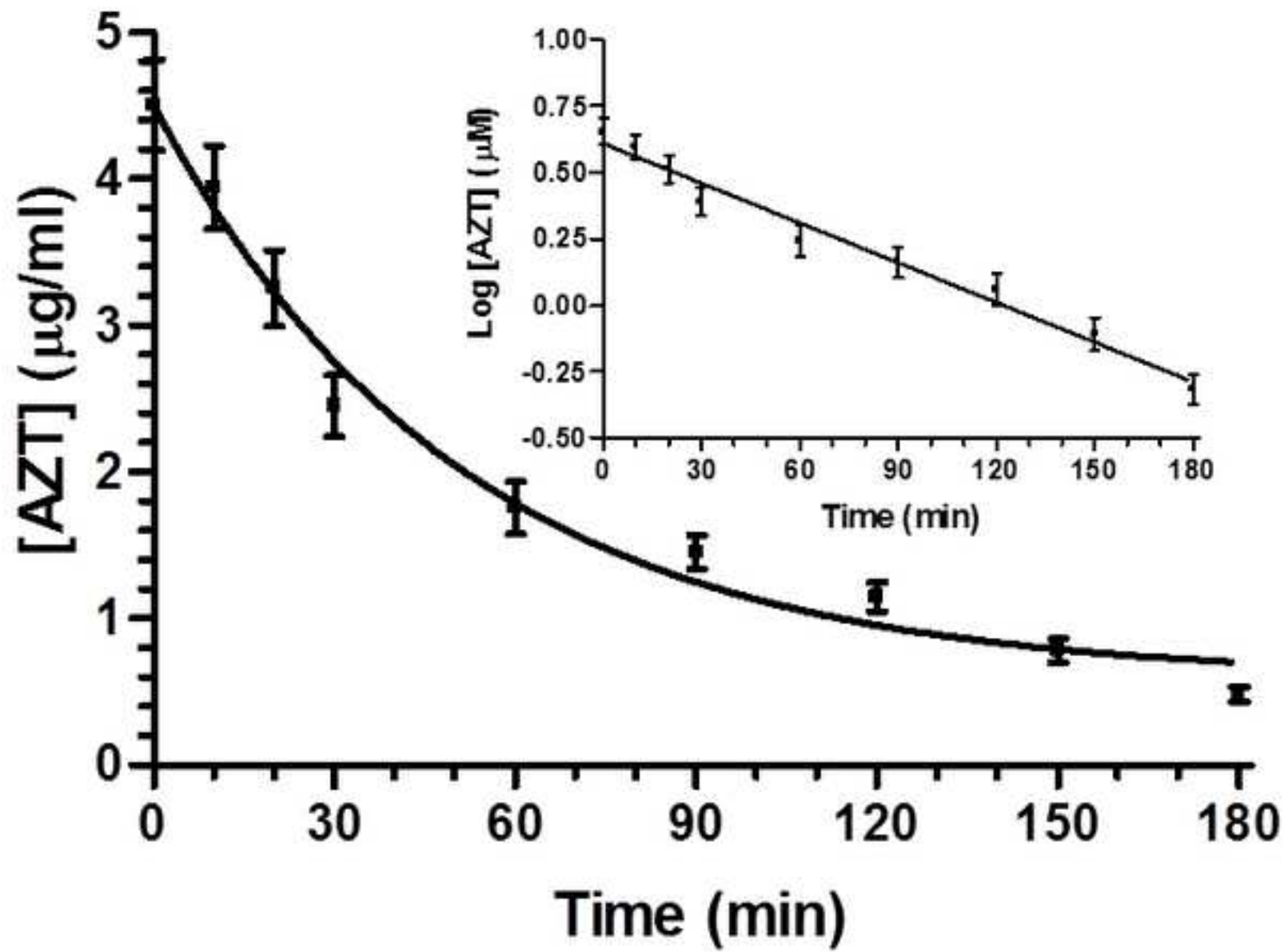


Figure 8
[Click here to download high resolution image](#)

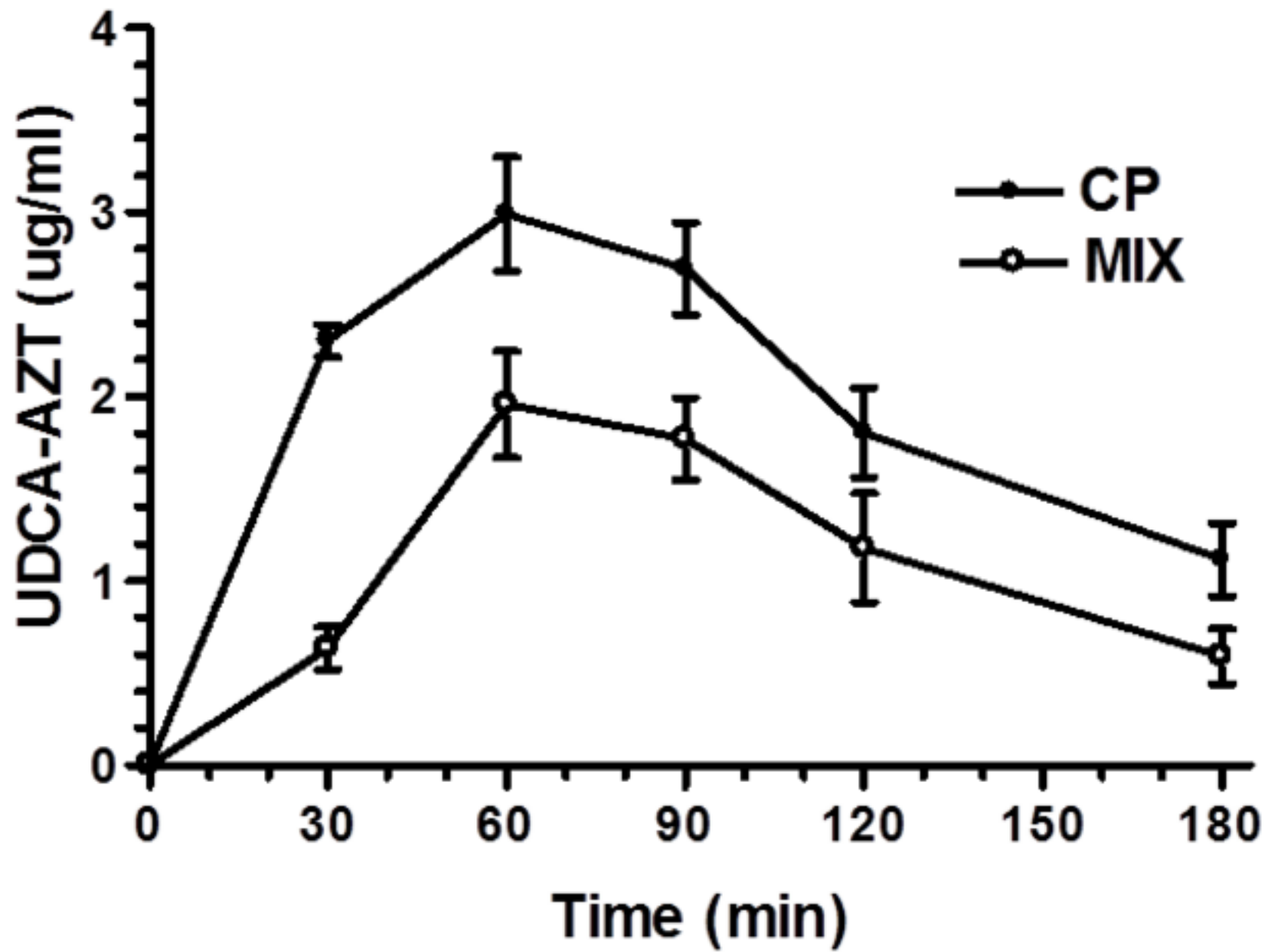
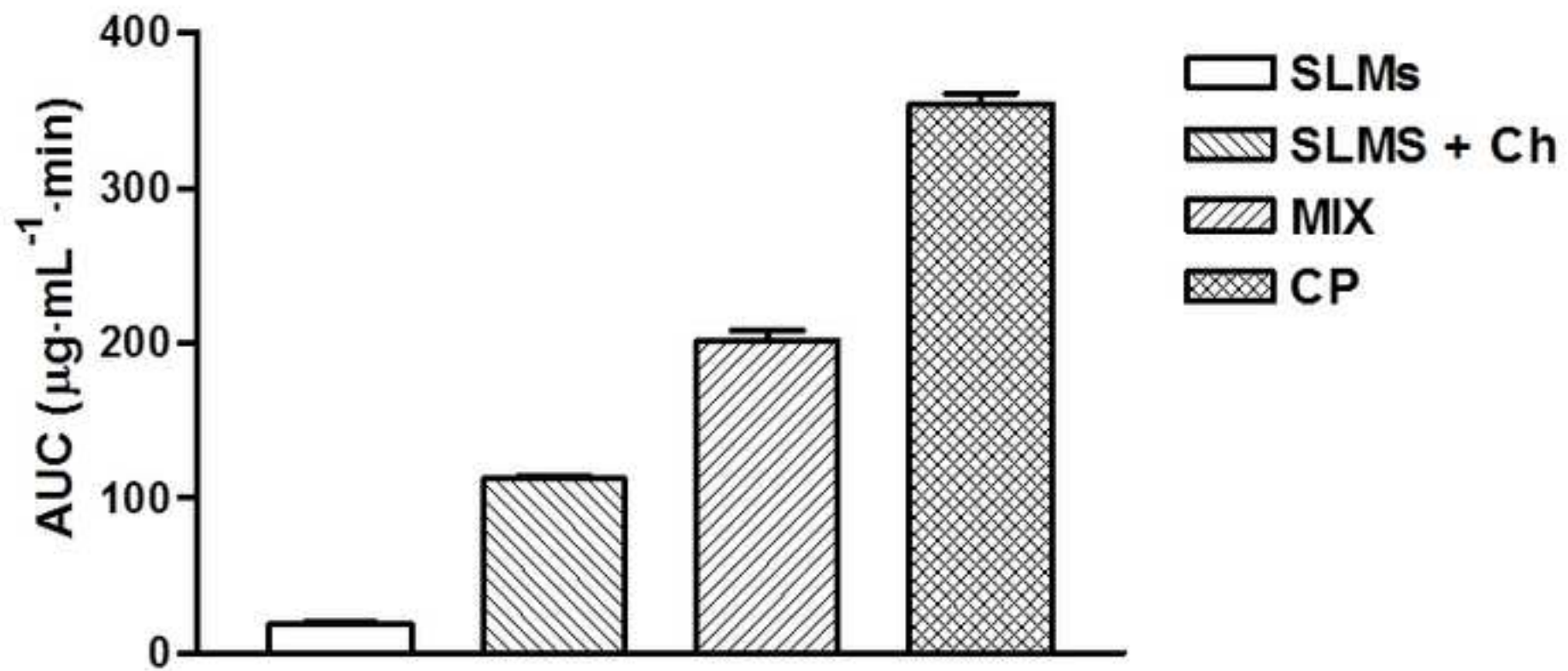
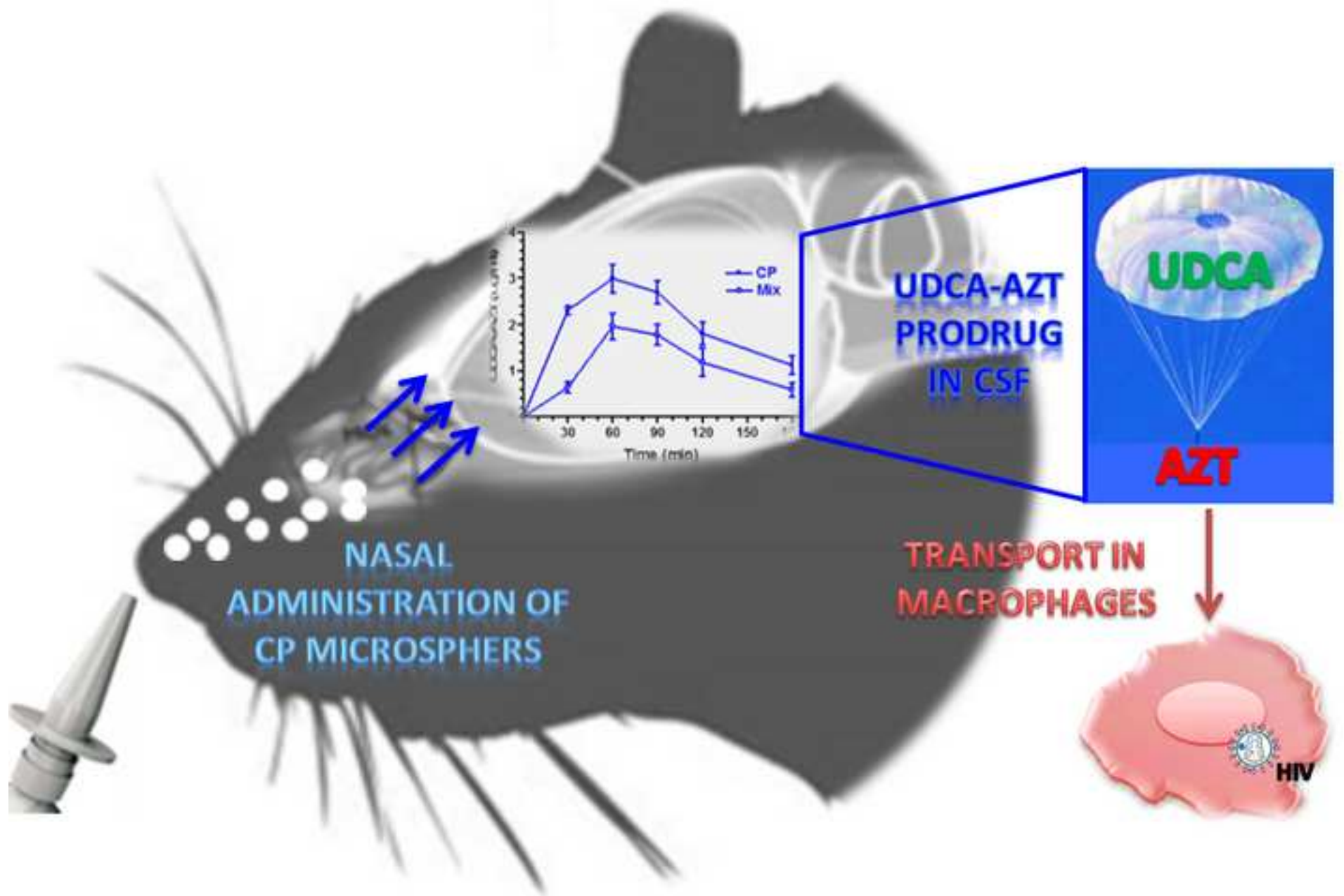


Figure 9
[Click here to download high resolution image](#)





Supplementary material

[Click here to download Supplementary file\(s\): Supplementary material.pdf](#)